

**DOT/FAA/TC-15/39**

Federal Aviation Administration  
William J. Hughes Technical Center  
Aviation Research Division  
Atlantic City International Airport  
New Jersey 08405

# **Current Capabilities for Icing Nowcasting and Forecasting in the Terminal Area**

November 2015

Final Report

This document is available to the U.S. public through the National Technical Information Services (NTIS), Springfield, Virginia 22161.

This document is also available from the Federal Aviation Administration William J. Hughes Technical Center at [actlibrary.tc.faa.gov](http://actlibrary.tc.faa.gov).



U.S. Department of Transportation  
**Federal Aviation Administration**

## **NOTICE**

This document is disseminated under the sponsorship of the U.S. Department of Transportation in the interest of information exchange. The U.S. Government assumes no liability for the contents or use thereof. The U.S. Government does not endorse products or manufacturers. Trade or manufacturers' names appear herein solely because they are considered essential to the objective of this report. The findings and conclusions in this report are those of the author(s) and do not necessarily represent the views of the funding agency. This document does not constitute FAA policy. Consult the FAA sponsoring organization listed on the Technical Documentation page as to its use.

This report is available at the Federal Aviation Administration William J. Hughes Technical Center's Full-Text Technical Reports page: [actlibrary.tc.faa.gov](http://actlibrary.tc.faa.gov) in Adobe Acrobat portable document format (PDF).

1. Report No. DOT/FAA/TC-15/39		2. Government Accession No.		3. Recipient's Catalog No.	
4. Title and Subtitle CURRENT CAPABILITIES FOR ICING NOWCASTING AND FORECASTING IN THE TERMINAL AREA		5. Report Date November 2015		6. Performing Organization Code	
		8. Performing Organization Report No.		10. Work Unit No. (TRAIS)	
7. Author(s) Scott Landolt and Marcia Politovich		9. Performing Organization Name and Address National Center for Atmospheric Research Foothills Laboratory 3450 Mitchell Lane Boulder, CO 80301		11. Contract or Grant No.	
12. Sponsoring Agency Name and Address U.S. Department of Transportation Federal Aviation Administration 1517 Arthur Avenue Lakewood, Ohio 44107		13. Type of Report and Period Covered Final Report		14. Sponsoring Agency Code AIR-100	
		15. Supplementary Notes The Federal Aviation Administration Aviation William J. Hughes Technical Center Aviation Research Division COR was James T. Riley.			
16. Abstract <p>The Federal Aviation Administration (FAA) has determined that there is a need for improvement in icing weather information, both on the ground and aloft, in terminal areas of airports. This is partly in response to a new rule, Title 14 Code of Federal Regulations Part 25.1420, which encompasses supercooled large drop conditions, including freezing rain and freezing drizzle either at the surface or aloft.</p> <p>The FAA has initiated a research project, Terminal Area Icing Weather Information for NextGen (TAIWIN), which will provide improved and modernized management of all terminal-area icing weather information for operational decision-making for both ground and in-flight icing conditions. TAIWIN will combine products for both ground and in-flight icing, including in situ sensors, weather satellites, weather radar, numerical weather prediction (NWP) models, nowcasting techniques, and enhanced or new technologies.</p> <p>The capabilities described in this report can help provide information on icing conditions within the terminal area. It will be important to assess the ability of each product to determine the presence, absence, and characteristics of icing conditions and to determine how to integrate the products (current, improved, and new) into a single algorithm for TAIWIN.</p>					
17. Key Words TAIWIN, Icing, SLD, Ground Icing, In-flight Icing, Freezing Rain, Freezing Drizzle, Terminal Area Icing, Aircraft Icing, Icing Sensors, Forecasting Icing Conditions, Detecting Icing Conditions.			18. Distribution Statement This document is available to the U.S. public through the National Technical Information Service (NTIS), Springfield, Virginia 22161. This document is also available from the Federal Aviation Administration William J. Hughes Technical Center at <a href="http://actlibrary.tc.faa.gov">actlibrary.tc.faa.gov</a> .		
19. Security Classif. (of this report) Unclassified		20. Security Classif. (of this page) Unclassified		21. No. of Pages 66	22. Price

## TABLE OF CONTENTS

EXECUTIVE SUMMARY	ix
1 INTRODUCTION	1
2 NATIONAL WEATHER SERVICE-PRODUCED FORECASTS AND WARNINGS	1
2.1 Airmen’s Meteorological Bulletin and Graphical Airmen’s Meteorological Bulletin	1
2.2 Significant Meteorological Information	4
2.3 Terminal Area Forecast	5
3 OBSERVATIONS	8
3.1 Automated Surface Observing Systems	8
3.2 Automated Weather Observing Systems	12
3.3 Automated Weather Sensor System	13
3.4 Runway/Roadway Surface Sensors	14
3.5 NEXRAD	14
3.6 Terminal Doppler Weather Radar	18
3.7 Commercial Radars	20
3.8 Microwave Radiometers	22
3.9 Satellite Products	23
3.10 The Global Aircraft Meteorological Data Relay and the Aircraft Communications and Reporting System	29
3.11 Tropospheric Airborne Meteorological Data Reporting	30
3.12 Combined Remote Sensors	31
4 NWP MODELS	31
4.1 NCEP Operational Models	31
4.2 NCEP Experimental Ensemble Forecast	34
5 ALGORITHMS	39
5.1 CIP and Forecasting Icing Products	39
5.2 LOWICE	41
5.3 System of Icing Geographic Identification in Meteorology for Aviation	42
5.4 Advanced Diagnosis and Warning System for Aircraft Icing Environments	44
5.5 Global Icing Forecast Products	45
6 DECISION SUPPORT SYSTEMS	45
6.1 Weather Support to Deicing Decision Making	45

	6.2 Canadian Airport Nowcasting Forecast System	46
7	SUMMARY	48
8	REFERENCES	50

## LIST OF FIGURES

1	AIRMET for icing and freezing level	2
2	Icing G-AIRMET	4
3	Icing SIGMET issued March 24, 2013	5
4	Example TAF	7
5	ASOS sensor layout	9
6	The BFGoodrich ice detector model 0872E3	10
7	Frequency of the BFGoodrich vibrating rod-icing sensor plotted against time	11
8	The Vaisala PWD22 optical present weather detection sensor	13
9	The Optical Scientific LEDWI sensor currently used on ASOS	13
10	Vaisala DRS511 road/runway surface sensor	14
11	TDWR locations	19
12	The Metek K-band MRR-2 radar	21
13	Reflectivity time-height cross section from the Metek MRR-2 radar	22
14	A Radiometrics model MP-3000A profiling radiometer	23
15	Merged GOES	27
16	CloudSat radar reflectivity cross-section from 2028–2029 UTC on November 5, 2006	29
17	VSREF forecasts of icing at 18,000 ft for 1800 UTC—July 16, 2012	35
18	NARRE-TL forecasts of icing at 18,000 ft for 1800 UTC— July 16, 2012	36
19	CIP analysis of forecast at 18,000 ft for 1800 UTC on July 16, 2012—from Aviation Digital Data Service flight path Java tool	37
20	Reliability plots for NARRE-TL and VSREF [41]	39
21	Performance statistics for FIP, CIP, and AIRMETs as a function of altitude	41
22	Example plots of estimated LWC and icing rate at 90 m AGL over the LOWICE Scandinavia domain	42
23	SIGMA algorithm icing index output	43
24	Vertical distribution of $POD_y$ and $POD_n$ values for ADWICE and FIP	44
25	The WSDDM real-time display for Denver International Airport	46
26	Schematic of CAN-Now	47
27	An Example of the CAN-Now situation chart for CYYZ	48

## LIST OF TABLES

1	NEXRAD Level III general products	16
2	TDWR products	20
3	Current GOES imager instrument characteristics	24
4	Current GOES sounder channels	25
5	NASA LaRC icing-related GOES products	26
6	NCEP model output relevant to diagnosing icing conditions	32

## LIST OF ABBREVIATIONS AND ACRONYMS

nmi	Nautical miles
ACARS	Aircraft Communications and Reporting System
ADWICE	Advanced Diagnosis and Warning System for Aircraft Icing Environments
AGL	Above ground level
AIRMET	Airmen’s Meteorological Bulletin
AMDAR	Global Aircraft Meteorological DATA Relay
AMSR	Advanced Microwave Scanning Radiometer
ASOS	Automated Surface Observing Systems
ATOVS	Advanced Television Infrared Observation Satellite Operational Vertical Sounder
AVHRR	Advanced Very High Resolution Radiometer
AWC	Aviation Weather Center
AWOS	Automated Weather Observing Systems
AWSS	Automated Weather Sensor System
CAN-Now	Canadian Airport Nowcasting Forecast System
CIP	Current Icing Product
CONUS	Continental United States
COSMO-EU	Consortium for Small Scale Modeling—Europe
CPR	Cloud Profiling Radar
DLR	German Aerospace Center
DWD	German Weather Service
EPI	Enhanced Present-Weather Indicator
FAA	Federal Aviation Administration
FIP	Forecast Icing Product
FZDZ	Freezing drizzle
FZRN	Freezing rain
G-AIRMET	Graphical Airmen’s Meteorological Bulletin
GDCP	GOES Derived Cloud Products
GFS	Global Forecast System
GOES	Geostationary Operational Environmental Satellite(s)
HCA	Hydrometeor classification algorithm
LAPS	Local Area Prediction System
LaRC	NASA Langley Research Center
LEDWI	Light Emitting Diode Weather Indicator
METAR	Aviation Routine Weather Report
MOG	Moderate or greater
MRMS	Multi-Radar Multi-Sensor
NAM	North American Mesoscale Forecast System
NARRE	North America Rapid Refresh Ensemble
NARRE-TL	North America Rapid Refresh Ensemble -Time Lagged
NCAR	National Center for Atmospheric Research
NCEP	National Centers for Environmental Prediction
NetCDF	Network Common Data Format
NEXRAD	Next-Generation Radar

NIRSS	NASA Icing Remote Sensing System
NOAA	National Oceanic and Atmospheric Administration
NSSL	National Severe Storms Laboratory
NWP	Numerical Weather Prediction
NWS	National Weather Service
PIREP	Pilot report
POD	Probability of detection
POES	Polar Orbiting Environmental Satellite
QPE	Quantitative precipitation estimate
RAP	Rapid Refresh
RASS	Radio acoustic sounding system
SIGMA	System of Icing Geographic Identification in Meteorology for Aviation
SIGMET	Significant Meteorological Information
SLD	Supercooled large droplet
TAF	Terminal Area Forecast
TAIWIN	Terminal Area Icing Weather Information for NextGen
TAMDAR	Tropospheric Airborne Meteorological Data Reporting
TDWR	Terminal Doppler Weather Radar
TRACON	Terminal Radar Approach Control
VIL	Vertically integrated liquid
VSREF	Very Short Range Ensemble Forecast
WMO	World Meteorological Organization
WRF	Weather Research and Forecasting
WSDDM	Weather support to deicing decision making

## EXECUTIVE SUMMARY

The Federal Aviation Administration (FAA) has determined that there is a need for improvement in icing weather information, both on the ground and aloft, in terminal areas of airports. This is partly in response to a new rule (Title 14 Code of Federal Regulations Part 25.1420) that encompasses supercooled large droplet conditions, including freezing rain and freezing drizzle (FZDZ), either at the surface or aloft. The Part 25.1420 rule would apply to airplanes with either: 1) a takeoff maximum gross weight of less than 60,000 lb, or 2) reversible flight controls. However, planning is underway for improved and modernized management of all terminal-area icing weather information for operational decision-making for both ground and inflight icing conditions.

In response to this need, the FAA has initiated a research project, Terminal Area Icing Weather Information for NextGen (TAIWIN), which will manage terminal-area icing weather information for operational decision-making for both ground and in-flight icing conditions. TAIWIN will combine products for both ground and in-flight icing, including in situ sensors, weather satellites, weather radar, Numerical Weather Prediction (NWP) models, nowcasting techniques, and enhanced or new technologies.

The first step in developing TAIWIN is determining what is already available for observing and forecasting both ground and in-flight icing conditions in the terminal area. This document describes available instruments, products, and systems, and summarizes their capabilities.

Many in situ sensors are already in use or available for diagnosing icing conditions in the terminal area. Surface-based sensors, such as those found on Automated Surface Observing Systems, Automated Weather Observing Systems, and Automated Weather Sensor Systems, have the capability to detect icing, either through the use of optical sensors or through direct detection of ice accretion on vibrating rod instrumentation. Though these systems have proven useful in the detection of icing conditions on the ground, their measurements are valid only at a single point. It has been observed that, particularly at larger airports, icing conditions (e.g., FZDZ) may vary dramatically over the terminal area, and in some cases only affect a portion of an airport.

Weather satellites have the capability to obtain measurements encompassing a large area. Significant research has gone into the development of satellite-based algorithms for detecting icing conditions. Scientists at the NASA Langley Research Center have developed algorithms specifically for use with current weather satellites to determine icing conditions in clouds. Satellite products observe conditions at or near cloud top, possibly incorporate information from NWP models, and apply algorithms based on meteorological principles to deduce icing conditions. Both the spatial and temporal resolution of weather satellites have steadily improved, and this bodes well for future use as part of TAIWIN.

Weather radars also provide measurements over terminal areas. Investigators have been working to develop algorithms for detection of icing and surface freezing precipitation using radar data, both in their previous form and now with the Next-Generation Radar (NEXRAD)

dual-polarization upgrades. The latter are particularly promising with respect to distinguishing types of freezing and frozen precipitation. Radar products are restricted to detecting conditions along the length of the radar beam, which gets higher and broader with distance from the radar.

NWP models can provide information on the ground and aloft, and their resolution can be increased to give better representations of potentially varying icing conditions within the terminal area. Numerous NWP model forecasts are available, though no current operational model is well-suited to TAIWIN. Improvements in spatial and temporal resolution will be needed, though this puts greater strain on computer resources to produce forecasts in a timely manner, and higher resolution can necessitate modifications to model physics to simulate the weather at finer scales. There may be value in using output in an ensemble mode to provide information on forecast probability or confidence.

Nowcasts, though highly valuable in the short term (0–2 hours depending on the weather phenomenon), tend to decrease in accuracy in the long term (more than 2 hours) because they rely solely on extrapolation and tracking of the current weather and do not account for changing conditions, speed, and weather type.

The capabilities described in this report can help provide information on icing conditions within the terminal area. Some, such as NEXRAD dual-polarization radar, though already in operational use, require further development and verification of algorithms tailored to the extraction of icing information, specifically the type of freezing and frozen precipitation. The automatic determination of FZDZ, either using existing or improved technology, would also make a valuable contribution. It will be important to assess the ability of each product to determine the presence, absence, and characteristics of icing conditions and to determine how to integrate the products (current, improved, and new) into a single algorithm for TAIWIN.

## 1. INTRODUCTION

The planned Terminal Area Icing Weather Information for NextGen (TAIWIN) will manage terminal-area icing weather information for operational decision-making for both ground and inflight icing conditions. The system will combine products of ground and inflight icing research; weather radar; remote and in situ sensors; and other new or enhanced technology.

The first step in developing TAIWIN is determining what is already available for observing and forecasting both ground and inflight icing conditions in the terminal area. This report describes instruments, products, and systems available, and summarizes their capabilities. However, it is not the purpose of this report to assess their quality or suitability for meeting TAIWIN requirements, which are in the process of being developed.

Some of the capabilities described in this document were developed specifically for the terminal area. Though most were not, they could still provide information useful to assess icing conditions in the terminal area. This document focuses on capabilities developed for the Continental United States (CONUS). However, some international systems have been included when the information was considered helpful and relevant to this review.

Finally, it should be noted that references to products and capabilities of specific commercial vendors do not imply endorsements.

## 2. NATIONAL WEATHER SERVICE-PRODUCED FORECASTS AND WARNINGS

### 2.1 AIRMEN'S METEOROLOGICAL BULLETIN AND GRAPHICAL AIRMEN'S METEOROLOGICAL BULLETIN

The Airmen's Meteorological Bulletin (AIRMET) was formerly designated a primary product for inflight icing forecasts. AIRMETs are issued by forecasters for the CONUS and Hawaii at the National Weather Service's (NWS's) Aviation Weather Center (AWC) in Kansas City, Missouri, and in Alaska by the Alaska Aviation Weather Unit. A primary product was defined by the NWS as an aviation weather product that meets all the regulatory requirements and safety needs for use in making flight-related aviation weather decisions (Flight Standards Information Management System, Order 8900.1, paragraph 3-2073; also, Aeronautical Information Manual, Section 7-1-3). However, the distinction between primary and supplementary products was eliminated as of April 3, 2014.

An AIRMET is a forecast for icing conditions of moderate or greater (MOG) severity not associated with convection and is meant to describe widespread conditions for at least 3000 square miles. However, because conditions may move across the forecast area, only a smaller area might be affected at any given time. AIRMETs are text products extending to 6 hours, and amendments are possible. The area is described as a dot-to-dot polygon, usually based on distances and directions from waypoints or specific latitudes and longitudes. An example is shown in figure 1.

```

WAUS45 KPCI 031445
SLCZ WA 031445
AIRMET ZULU UPDT 2 FOR ICE AND FRZLVL VALID UNTIL 032100
AIRMET ICE...MT
FROM 50NNW ISN TO 80SW DIK TO 20NNW SHR TO 80E DLN TO 20N HVR TO
50NNW ISN
MOD ICE BTN 120 AND FL220. CONDS ENDG 18-21Z.
FRZLVL...RANGING FROM 085-170 ACRS AREA
 120 ALG 30ESE GEG-30N LKT-70ESE DLN-20NE SHR-60WSW DIK
 160 ALG 70SSE LKV-80NNE FMG-30S BAM-30NW HVE-30SE HVE-50S HVE-
 30WNW BTY
 160 ALG 40S DMN-60SSE SJN-60SSW RSK-RSK-50SE HBU-20W PUB-
 40ESE LAA

```

**Figure 1. AIRMET for icing and freezing level**

This AIRMET is translated as follows:

*>Forecast for the 3rd day of the month that this AIRMET was issued (name of month is not included in AIRMET) at 1445 UTC for Salt Lake City area.*

*>AIRMET Zulu (for icing), update 2 for ice and freezing level valid until 2100 on August 3.*

*>AIRMET for icing in Montana.*

*>From 50 nautical miles (nmi) north northwest of Williston, ND to  
80 nmi southwest of Dickinson, ND to  
20 nmi north-northwest of Sheridan, WY to  
80 nmi east of Dillon, MT to  
20 nmi north of Haver, MT to  
50 nmi north-northwest of Williston, ND.*

*>Moderate icing between 12,000–22,000 ft (altitudes below 18,000 ft are given in hundreds of ft, above that they are referred to as Flight Levels or FLxxx, and are again in hundreds of feet). Conditions ending 1800–2100Z.*

*>Freezing level ranging from 8,500–17,000 ft across the area.*

*>Details: 12,000 ft along a line  
30 nmi east-southeast of Spokane, WA to  
30 nmi north of the Salmon, ID VOR to  
70 nmi east-southeast of Dillon, MT to  
20 nmi northeast of Sheridan, WY, to  
60 nmi west-southwest of Dickenson, ND.*

*>16,000 ft along a line  
70 nmi south-southeast Lakeview, OR to  
80 nmi north-northeast of the Reno, NV VOR to  
30 nmi south of the Battle Mtn, NV VOR to  
30 nmi northwest of Haver, MT to  
30 nmi southeast of Haver, MT to  
50 nmi south of Haver, MT to  
30 nmi west-northwest of Beatty, NV.*

*>16,000 ft along a line  
40 nmi south of DMN to  
60 nmi south-southeast of SJN to  
60 nmi south-southwest of Rattlesnake/Farmington, NM,  
and another line from  
Rattlesnake/Farmington, NM to  
50 nmi southeast of the Gunnison, CO VOR to  
20 nmi west of Pueblo, CO to  
40 nmi east-southeast of Lamar, CO.*

Graphical Airmen's Meteorological Bulletins (G-AIRMETs) became operational in March 2010. These are graphical depictions of the text AIRMET with polygons drawn and tags added to describe details, such as top and base, and movement of weather volume. The G-AIRMET corresponding to the AIRMET in figure 1 is shown in figure 2 and is outlined by the blue-dotted line. The symbols indicate that the G-AIRMET is for moderate icing, and the valid time is shown in the lower left corner. G-AIRMETs are issued every 3 hours with 0-, 3-, 6-, 9-, and 12-hour "snapshot" images.

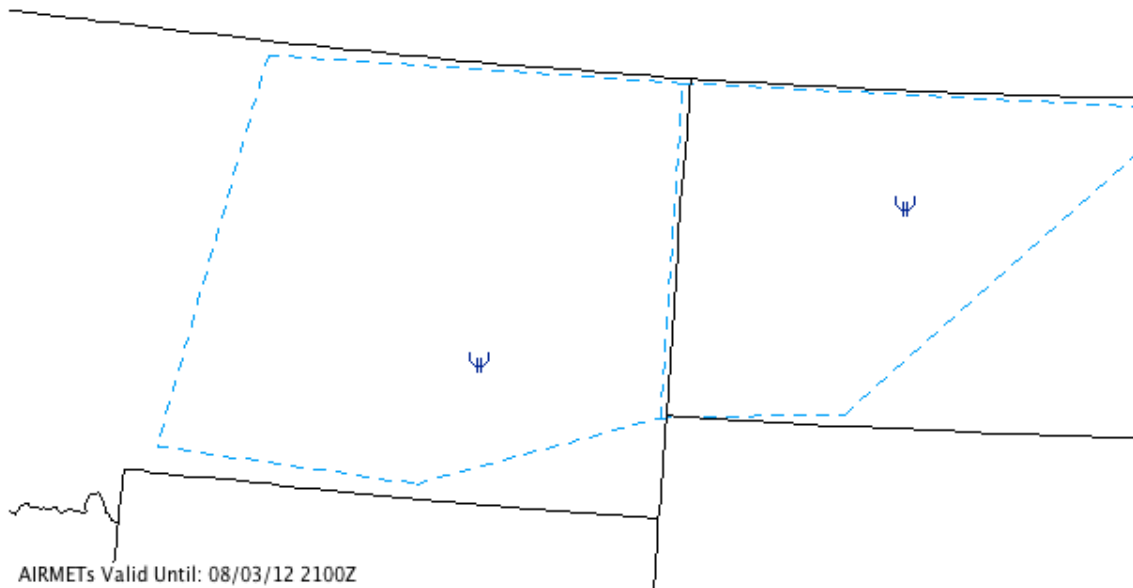


**Figure 2. Icing G-AIRMET**

## 2.2 SIGNIFICANT METEOROLOGICAL INFORMATION

Icing Significant Meteorological Information (SIGMET) is an immediate advisory of severe icing. It has the same 3000 square mile minimum size as an AIRMET but is issued as needed, typically when at least one pilot reports severe icing from the aircraft. The forecaster, after receiving a severe icing pilot report (PIREP), consults various information sources (such as nearby PIREPs, Numerical Weather Prediction model [NWP] outputs, radar maps, satellite imagery, and surface reports), determines whether the weather conditions appear to warrant a SIGMET, and, if so, determines the likely extent in time and space of the severe condition. Then the SIGMET is issued. However, on occasion, a forecaster will issue a SIGMET when conditions are considered conducive to severe icing but no severe PIREP has been received. An example of this occurred February 28, 2006 for a SIGMET that covered an area close to the Salt Lake City Airport. Because this was a busy air traffic area, and InFlight Icing Product Development Team staff did not note a PIREP, they asked the AWC icing forecaster on duty at the time (with permission from the AWC lead forecaster) about his reasoning. The forecaster explained that after consulting some of the NWP models, he noticed an area of unusually high liquid water content in an appropriate temperature range and considered such a warning justified. A SIGMET closes the airspace to all aircraft, even those certified for flight into icing conditions because a “severe” icing situation is defined as one for which no ice protection system is effective. However, complete closure of the airspace does not consistently happen in practice for a variety of reasons. For example, the SIGMET may not have been passed along to air traffic controllers, or controllers may have noted other aircraft traversing the area and consider it safe. However, it is generally difficult to verify SIGMETs using PIREPs because most aircraft will avoid, or will be directed to avoid, the area.

By studying flight tracks in the vicinity of icing SIGMETs and comparing them to days without SIGMETs, it was found that when icing SIGMETs were issued they had a noticeable impact on air traffic routing, especially in busy areas [1]. The Salt Lake City SIGMET was one of the examples they cited. However, the overall impact of icing SIGMETs is likely small because SIGMETs are not commonly issued. Only seven icing SIGMETs were issued from October 2011–February 2012.

An example of a SIGMET is shown in figure 3.

```
SIGMET XRAY 1 VALID UNTIL 242133
WV VA NC KY TN
FROM 50WSW BKW TO 30NNW
LYH TO 40N CLT TO VXV TO
50WSW BKW
OCNL SEV RIME/MXD ICGICIP
BTN 080 AND 160 RPTD BY ACFT
CONDS CONTG BYD 2133Z
```

**Figure 3. Icing SIGMET issued March 24, 2013**

This SIGMET is interpreted as follows:

- >*SIGMET XRAY 1 (internal numbering system) valid until (month not specified) 2133Z*
- >*For West Virginia, Virginia, North Carolina, Kentucky, and Tennessee*
- >*From 50 nmi west-southwest of Beckley, WV to 30 nmi west-northwest of Lynchburg, VA, to 40 nmi north of Charlotte, NC, to Knoxville, TN, to 50 nmi west-southwest of Beckley, WV*
- >*Occasional severe rime/mixed icing in cloud in precipitation between 8,000–16,000 ft. Reported by aircraft.*
- >*Conditions continuing beyond 2133Z.*

### 2.3 TERMINAL AREA FORECAST

The Terminal Area Forecast (TAF) is a prediction of aviation weather activity at airports. A TAF applies to a circular area with a 5-mile radius from the center of the airport runway complex. This is significant, for it allows the forecaster to take into account local variations in terrain, proximity to large bodies of water, and small-scale weather patterns that are not included in the AIRMETs and other large-scale forecasts. TAFs are issued 20–40 minutes prior to each of the four daily forecast periods at 0000, 0600, 1200, and 1800 UTC. Forecast windows vary, but, generally, TAFs apply to a 9- or 12-hour forecast, though some TAFs cover an 18- or 24-hour period. As of November 5, 2008, TAFs for some major airports cover 30-hour periods. Weather conditions at the covered airports are carefully monitored and amendments are issued if needed, following specific criteria.

The TAF includes forecasts for:

- Federal Aviation Administration (FAA) towered airports
- Federally contracted towered airports
- Non-federal towered airports
- Non-towered airports

TAFs are produced by human forecasters in the United States<sup>1</sup>. The weather forecaster responsible for a TAF is not usually stationed at the location to which the TAF applies, but at an assigned Center Weather Service Unit or Weather Service Forecast Office.

There are four types of lines in a TAF. The first gives location, valid time, and prevailing weather for that time until the next line of the forecast. A BECMG (becoming) line indicates that, in the period given, the weather is expected to change from the previous line to that line; an FM (from) line indicates that, after the given time, the weather will be what the line states; a TEMPO line indicates a temporary or intermittent condition, such that the total time spent in those conditions will not add up to more than half the period covered by the TAF. There are also trends, which are truncated versions of a TAF, giving the expected conditions in a 2-hour period following the issue of an observation.

The weather information includes wind, visibility, weather, sky condition, and optional data (e.g., wind shear). Icing-relevant parameters are included in the weather information and include types of precipitation, such as:

- DZ - Drizzle
- RA - Rain
- SN - Snow
- SG - Snow Grains
- IC - Ice Crystals
- PL - Ice Pellets
- GR - Hail
- GS - Small Hail or Snow Pellets (less than 1/4" diameter)
- UP - Unknown Precipitation (automated stations only)

There may also be a probability forecast field that provides the probability of thunderstorms or other precipitation events occurring, along with the associated weather conditions. Probabilities are in 20% ranges (e.g., PROB40 means a probability between 30% and 50%). Changes and trends within the forecast period are also indicated, as are temporary conditions (less than one hour at a time, and less than one half of the forecast). An example is shown in figure 4.

---

<sup>1</sup> TAFs are available on the Internet at <http://aspm.faa.gov/>.

KDEN 031900Z 0319/0424 29010G16KT P6SM FEW090 SCT140 BKN250  
FM040100 35007KT P6SM FEW100 BKN140  
FM040500 02016G26KT P6SM FEW040 SCT100 SCT140  
FM040900 02012KT P6SM SCT025 BKN040  
FM041600 05010KT P6SM FEW025 SCT040  
FM041900 12012KT P6SM FEW050 SCT100

**Figure 4. Example TAF**

The translation of this TAF is:

*>Forecast for Denver International Airport 3rd day of the month that this TAF was issued (month not identified) 1900Z for 3rd day of month 1900Z through 4th day of month 2400Z, present weather: winds 290° at 10 kt gusting to 16 kt, visibility 6 statute miles. Few clouds at 9000 ft, scattered clouds at 14,000 ft (all heights above ground level [AGL]), broken clouds at 25,000 ft*

*>From 4th day of the month 0100Z conditions will be: winds 350° at 7 kt, visibility 6 statute miles, few clouds at 10,000 ft, broken clouds at 14,000 ft*

*>From 4th day of month 0500Z conditions will be: winds 20° at 16 kt gusting to 26 kt, visibility 6 statute miles, few clouds at 4000 ft, scattered clouds at 10,000 ft, scattered clouds at 14,000 ft*

*>From 4th day of month 0900Z conditions will be: winds 20° at 12 kt, visibility 6 statute miles, scattered clouds at 2500 ft, broken clouds at 4000 ft*

*>From 4th day of month 1600Z conditions will be: winds 50° at 10 kt, visibility 6 statute miles, few clouds at 2500 ft, scattered clouds at 4000 ft*

*>From 4th day of month 1900Z conditions will be: winds 120° at 12 kt, visibility 6 statute miles, few clouds at 5000 ft, scattered clouds at 10,000 ft*

*(Note that on this day, Denver had considerable smoke in the air from various wildfires in the western states)*

The pilot typically uses a TAF until he is close enough to his final destination to assume that current weather reports will accurately represent the conditions he will encounter on landing the aircraft. In addition, the pilot may use current weather reports at his destination airport issued while en route to assess the accuracy of the TAF.

There are few verification studies of TAFs. The NWS's Southern Regional Headquarters launched an online verification tool in 2001 that, in addition to ceiling and visibility information, included thunderstorms, rain, snow, freezing precipitation, and fog. Results have not been

published in the open literature. Other TAF verifications (not just from the United States but around the world) have been published, but only for ceiling and visibility parameters.

### 3. OBSERVATIONS

#### 3.1 AUTOMATED SURFACE OBSERVING SYSTEMS

The Automated Surface Observing Systems (ASOS) were designed by the FAA and the NWS to report the standard surface meteorological conditions. These conditions include temperature; relative humidity; pressure; ceiling; visibility; wind speed and direction; precipitation type; and liquid-equivalent precipitation. The ASOS sensor layout is shown in figure 5. ASOS reports these conditions every 5 minutes, though Aviation Routine Weather Reports (METARs) are typically generated from them only once every hour. The 1-minute data can be obtained from ASOS, but they have not gone through the quality control algorithms that the 5-minute data have.

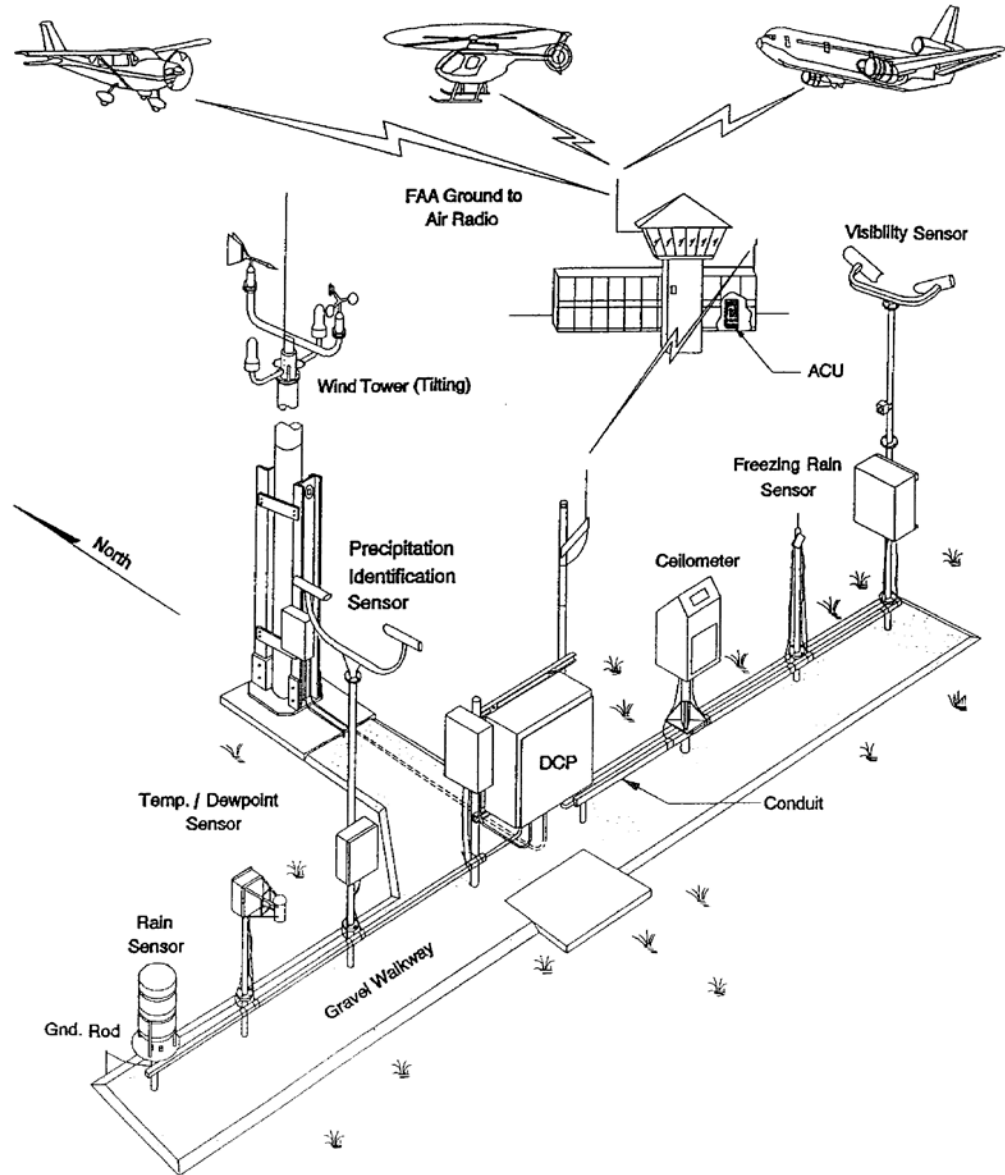
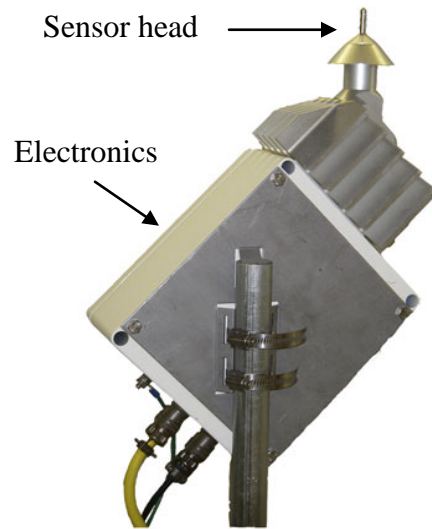


**Figure 5. ASOS sensor layout**

ASOS in its current form has the capability for detecting freezing rain (FZRN) at the surface using the BF Goodrich<sup>®</sup> ice detector<sup>2</sup> (see figure 6). This sensor operates by vibrating a metal rod pointed vertically in the air. As ice accretes on the metal rod, the vibration of the rod decreases from its nominal value of 40,000 Hz (see figure 7). In figure 7, the large dip infrequency suggests a FZRN event, whereas the smaller dips are either freezing drizzle (FZDZ) events or short-lived FZRN events. This drop in frequency is related directly to the amount of accretion through the equation:  $Th = 0.0004(FC)$ , where  $Th$  is the ice thickness in centimeters and  $FC$  is the change in frequency of the vibrating rod between measurements [2]. Because of the occasional noise

<sup>2</sup> These icing sensors are also installed on many commercial aircraft to warn pilots of icing conditions. There is as yet no capability to transmit this inflight information to a ground station or other aircraft.

observed in the sensor, ASOS requires that the frequency drop below 39,972 Hz before any freezing precipitation conditions will be reported. When the frequency stops decreasing or a frequency of 39,400 Hz is reached, a heat cycle is triggered and the ice is melted from the vibrating rod, bringing the frequency back to its baseline value of 40,000 Hz.



Model 0872E3 (c) 2007 Campbell Scientific (Canada) Corp.

**Figure 6. The BFGoodrich ice detector model 0872E3**

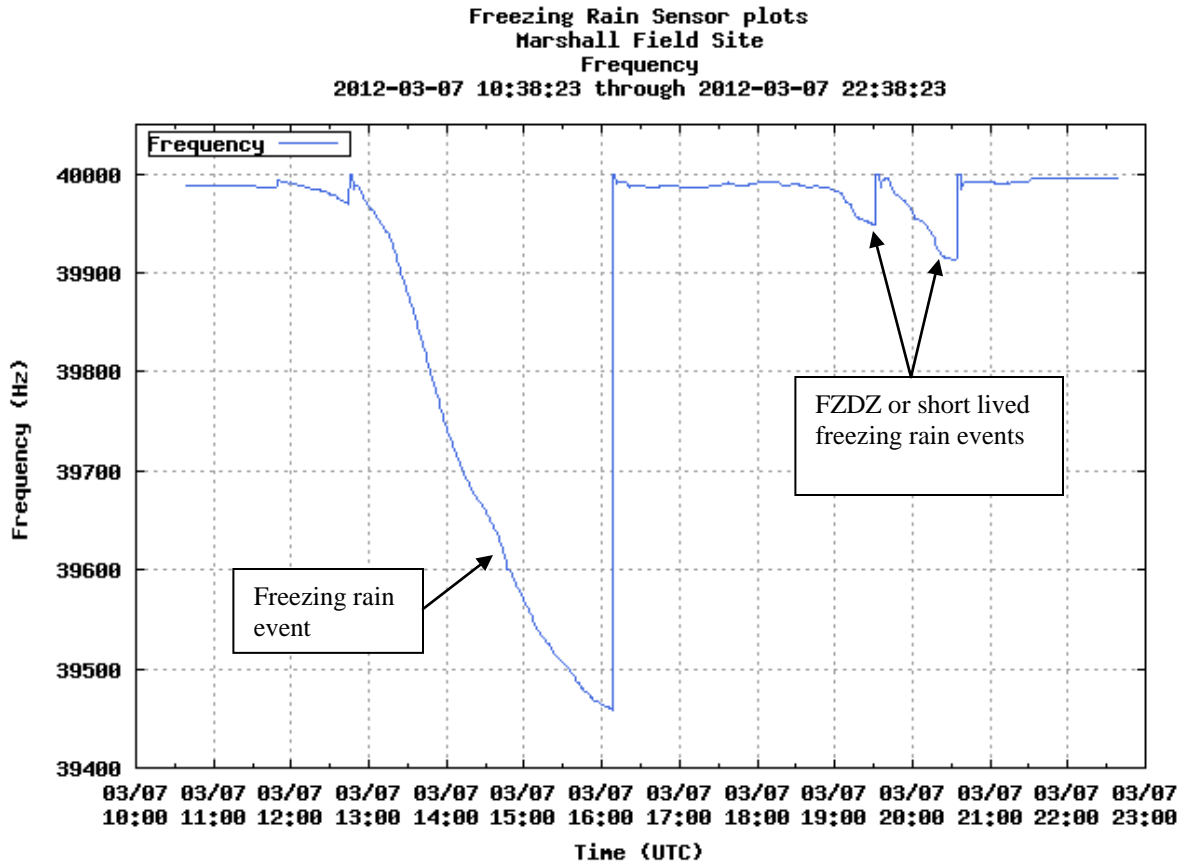


**Figure 7. Frequency of the BFGoodrich vibrating rod-icing sensor plotted against time**

The BF Goodrich ice detector was evaluated for its capabilities in detecting FZRN, FZDZ, and freezing fog during its original testing. The algorithm for detecting FZRN was incorporated into ASOS as soon as the sensor became operational; the FZDZ algorithm was not. Incorporation of this algorithm (developed by Ramsey) apparently became enmeshed in the replacement in ASOS of another instrument, the Light Emitting Diode Weather Indicator (LEDWI) with the Enhanced Present-Weather Indicator (EPI). According to discussions with NWS personnel on the ASOS Test Review Board by one of the authors, the EPI performed well in extensive testing, but narrowly failed to meet the specification for detection of ice pellets. This, now combined with funding issues, has resulted in the EPI not being accepted. This has been suggested as a reason for the delay in the incorporation of the FZDZ algorithm into the ASOS software, but this would seem to be a misunderstanding because the FZDZ algorithm was developed and evaluated for the LEDWI (although it could be modified to work with the EPI). With regard to freezing fog, its presence is inferred by ASOS, but not measured directly using the FZRN sensor. For ASOS to report freezing fog, visibility must be less than 5/8 of a mile and the temperature must be below freezing.

Though the FZRN detection algorithm on ASOS has proven to be robust, there are two drawbacks worth noting. First, wet snow can adhere to the vibrating rod, causing a decrease in frequency that can cause false reports of freezing precipitation. To get around this, ASOS will

not report freezing precipitation if the present weather sensor (LEDWI) is reporting snow. Second, the FZRN sensor can only operate over a set range of frequencies. If the frequency drops to 39,400 Hz, the sensor must initiate a de-icing cycle by heating the vibrating rod to melt the ice and return the frequency to its nominal vibrating frequency of 40,000 Hz. Because the sensor was heated above freezing to melt the ice, it must cool below freezing to begin accreting ice again. This process is usually ~30 minutes, during which time the sensor is too warm to accrete ice. It can, however, take up to several hours for the temperature of the rod to cool sufficiently if the ambient temperature is close to 0°C. This means that FZRN may be falling and not detected/reported by the sensor. There is a delay in the ASOS algorithm that allows FZRN to be reported for a certain period after the heating cycle is initiated (~10 minutes), but the delay is not related to intensity nor ambient air temperature. By examining a long-term dataset from the FZRN sensor along with local air temperature and wind speed, a relationship of the cooling rate of the vibrating rod to these parameters could likely be derived and a better, more dynamic reporting scheme for freezing precipitation during heating cycles of the FZRN sensor could be determined.

### 3.2 AUTOMATED WEATHER OBSERVING SYSTEMS

The Automated Weather Observing Systems (AWOS), of which there are several types with varying capabilities, were designed primarily for use at smaller airports (i.e., airports that serve more of the general aviation community). Unlike ASOS systems, which are standardized with identical components at each site, AWOS systems are non-standardized and the sensors vary depending on the distributor that installs the systems. AWOS generates real-time weather reports, updated every minute. These weather reports are made available to airport personnel via displays on operator terminals and to pilots via high-quality, digitized voice transmissions using a VHF frequency or voice-capable NAVAIID. AWOS reports are also available by telephone for flight planning and can be sent to the FAA's Weather Network for flight-planning purposes. In some instances, depending on the funding available, AWOS data are also made available via METAR format if communication lines can be installed to the AWOS site.

Currently, there are seven different types of AWOS systems available, depending on the measurements required by the airport: AWOS I, II, III, IIIP, IIIT, IIIPT, and IV. In some instances, AWOS IV is also referred to as AWOS PTZ. Of the seven systems, only the AWOS IV systems have the capability to report freezing precipitation. Because various manufacturers are allowed to install these units, not all AWOS sensors are the same. For example, AWOS stations may or may not use the BF Goodrich ice detector discussed in section 3.1. An optical present weather sensor, such as the Vaisala PWD22 (see figure 8), may be used to report freezing precipitation. ASOS uses the LEDWI (see figure 9) to determine present weather<sup>3</sup>.

---

<sup>3</sup> A list of surface stations with ASOS or AWOS can be found at <http://weather.rap.ucar.edu/surface/stations.txt>.



**Figure 8. The Vaisala PWD22 optical present weather detection sensor**



**Figure 9. The Optical Scientific LEDWI sensor currently used on ASOS**

### 3.3 AUTOMATED WEATHER SENSOR SYSTEM

The Automated Weather Sensor System (AWSS) is an enhanced version of the AWOS that also provides minute-by-minute weather observations. The AWSS is essentially a duplicate of the ASOS system, but is marketed solely by All Weather Inc. The AWSS uses some of the advanced algorithms developed for the ASOS system to produce an expanded suite of meteorological products. Observations include visibility; ceiling height; present weather type; wind speed and direction; freezing precipitation measurements; precipitation amounts; temperature; humidity; and atmospheric pressure. Weather observers may edit automatically generated weather data and daily and monthly summary reports, and manually generate special weather reports. In the case of freezing precipitation detection, AWSS uses the same BF Goodrich ice detector as ASOS. Determination of which airports get AWSS or AWOS systems is largely determined by money available for the system. Better-funded airports tend to have the higher-level AWOS or AWSS systems.

### 3.4 RUNWAY/ROADWAY SURFACE SENSORS

A new generation of runway and roadway surface sensors have been installed at various airports over the past several years. These sensors are embedded in the runway pavement and can directly measure water, snow, and ice buildup on the surface of the runway (see figure 10). In the absence of any other type of sensor, these sensors can provide valuable information on the presence of near-surface icing conditions in the immediate vicinity of aircraft anywhere on the airfield. Determination of ice buildup on runway and taxiway surfaces is completed using optical, electrical conductivity, and electrochemical polarizability measurements, which, when combined, can give an estimate of ice thickness and risk of ice formation. The surface sensors can also assist in determining the amount of deicing agent needed to clear the runway surface of ice. These sensors are manufactured and maintained by private vendors under contract to the FAA.



**Figure 10. Vaisala DRS511 road/runway surface sensor**

### 3.5 NEXRAD

The NEXRAD network consists of 159 10-cm (S-band) Doppler weather radars operated by the NWS. The technical name for the radars is WSR-88D, which stands for Weather Surveillance Radar, 1988, Doppler. NEXRAD operates in two basic modes, selectable by the operator: a slow-scanning clear-air mode for analyzing air movements when there is little or no activity in the area, and a precipitation mode, which has a faster scan for tracking active weather. There are several scan strategies within each mode, and complete volume scans take 4.5–10 minutes, depending on the scan type. The coverage of the volume scans for elevations below 10,000 ft is fairly good in the midwest and east, but coverage in the western United States is not as good because of terrain blockage. Range resolution is 1 km and azimuthal resolution is 1°. True range-height indicator scans are not completed; vertical cross sections can be constructed using the azimuthal scans, but their vertical resolution is generally too coarse to be of use in evaluating detailed cloud characteristics.

NEXRAD facilities were not designed to support terminal-area aviation operations; therefore, the radars may or may not be in suitable locations for supporting TAIWIN. The coverage of the volume scans for elevations below 10,000 ft varies significantly with terrain. As for near-surface sensing, the center of the 0.5° lowest-elevation scan rises 530 ft for every 10 nmi from the radar (not including earth curvature, which will increase this rise), reducing the ability for on-field

precipitation identification and tracking. For example, to adequately detect gust fronts, providing useful surface velocity data, a NEXRAD must operate within roughly 55 nmi of the airport [3].

NEXRAD data are available in a variety of formats. Level II data are the raw reflectivity, mean radial velocity, and spectrum width (velocity variance) “moment” data from the individual radar data processors (there is no Level I). Each dataset contains up to fourteen elevation angles; each tilt contains 360 radials with an azimuthal resolution of 1°. The radial resolution is 1 km for reflectivity and 250 m for both radial velocity and spectrum width. Sources for real-time Level II data include the Integrated Robust Assured Data Services of the University of Oklahoma<sup>4</sup>, Unidata (serving the university community), and others. Costs and restrictions on redistributing the data depend on the source.

Various algorithms ingest the Level II data to provide quality control, clutter filtering, and weather products. Level III General Products from NWS are listed in table 1. It may seem tempting to use vertically integrated liquid (VIL) to identify icing environments [4]. The VIL is calculated based on a relationship between radar reflectivity factor and mass of raindrops; the size distribution of those raindrops is assumed exponential. A cloud with high concentrations of small drops dominating the total liquid water content (which is generally the case in wintertime icing environments) could either be below the radar detection limit or, because reflectivity is dominated by the larger sizes (a sixth-power dependence on drop diameter), the liquid water estimate would be highly inaccurate. Therefore, the practical use of VIL to describe the icing environment is limited.

---

<sup>4</sup> Website located at <https://www.irads.net>.

**Table 1. NEXRAD Level III general products**

Field Name	Description
Base Reflectivity	Echo intensity (reflectivity) measured in dBZ. Images in Precipitation Mode are available at four radar tilt angles, 0.5°, 1.45°, 2.40°, and 3.35° (with slightly higher tilt angles in Clear Air Mode). The maximum range is 124 nmi.
Composite Reflectivity	Maximum reflectivity from the four tilt angles.
Base Radial Velocity	Velocity (in kt) either toward or away from the radar (in a radial direction) for just two tilt angles, 0.5° and 1.45°.
Storm Relative Mean Radial Velocity	As for Base Radial Velocity, but with the mean motion of the storm subtracted out, for all tilt angles.
VIL <sup>5</sup> Water	VIL is the amount of liquid water that the radar estimates in a vertical column of the atmosphere for an area of precipitation in kg m <sup>-2</sup> . The VIL values are computed for each 2.2 x 2.2 nm grid box for each elevation angle within a 124 nm radius of the radar, then vertically integrated.
Echo Tops	The maximum height of reflectivity ≥18.5 dBZ. The radar will not report echo tops <5000 ft or >70,000 ft.
Storm Total Precipitation	Estimated accumulated rainfall, continuously updated, since the last 1-hour break in precipitation.
One Hour Running Total Precipitation	Estimated 1-hour precipitation accumulation on a 1.1 x 1.1 nm grid.
Velocity Azimuth Display (VAD) Wind Profile	The VAD Wind Profile image presents snapshots of the horizontal winds at different altitudes above the radar. These wind profiles are spaced 6–10 minutes apart and are plotted in knots using the standard station model.

Additional precipitation accumulation products and storm characteristic information (such as mesocyclone) are available through various sources. Level III products are updated every 6 minutes if the radar is in precipitation mode, or every 10 minutes if the radar is in clear-air mode. The full suite of Level III products are available on the NOAAPORT satellite broadcast in real time<sup>6</sup>.

NEXRAD sites were upgraded in 2010 to add vertical polarization to the current horizontal radar waves<sup>7</sup>. This dual polarization upgrade allows the radar to estimate hydrometeor shape and, therefore, potentially distinguish between rain, drizzle, hail, and snow; horizontally polarized

<sup>5</sup> An excellent description of how VIL is calculated can be found at the Oklahoma Climatology Website: <http://okfirst.mesonet.org/train/nids/VILguide.html>

<sup>6</sup> Visit [http://www.nws.noaa.gov/tg/pdf/noaaport\\_radar\\_products.pdf](http://www.nws.noaa.gov/tg/pdf/noaaport_radar_products.pdf)

<sup>7</sup> For the upgrade schedule, visit <http://www.roc.noaa.gov/WSR88D/PublicDocs/DualPol/DPSchedule.pdf>.

radars cannot make this distinction, which is why they cannot distinguish precipitation type using reflectivity alone.

Dual-polarization data will be available on the Level II datastream<sup>8</sup> and on Level III products<sup>9</sup>. Reference 5 offers an excellent assessment of the potential of NEXRAD dual-polarization products.

A hydrometeor classification algorithm (HCA) using dual-polarization information has been incorporated into the Level II datastream. This provides an assessment of the type of hydrometeors (water drops or ice crystals, including ice crystal type) detected by the radar. However, the NEXRAD HCA has been demonstrated to perform poorly for winter hydrometeor types [6]. This is an area needing further research and development.

Polarization-based or enhanced outputs available for various radar tilt angles include:

- Differential reflectivity,  $Z_{dr}$ : The ratio of the reflected vertical and horizontal power returns as  $ZV/ZH$ .
- Correlation coefficient,  $\rho_{dp}$ : The correlation between the reflected horizontal and vertical power returns; a good indicator of regions with a mixture of precipitation types, such as rain and snow.
- Specific differential phase,  $K_{dp}$ : A comparison of the returned phase difference between the horizontal and vertical pulses. This change in phase is caused by the difference in the number of wave cycles (or wavelengths) along the propagation path for horizontally and vertically polarized waves.
- Hydrometeor classification

The Multi-Radar Multi-Sensor (MRMS) system was initially developed from a joint interagency initiative [7 and 8]. The objectives of MRMS research and development are: 1) to develop a meteorological platform for assimilating different observational networks toward creating high spatial and temporal resolution multi-sensor quantitative precipitation estimates (QPEs) for flood warnings and water resource management, and 2) to develop a seamless high-resolution national 3-D grid of radar reflectivity for severe weather detection, data assimilation, NWP model verification, and aviation product development. Therefore, the MRMS system is both a user and provider of NEXRAD data. A real-time MRMS system has been implemented at the University of Oklahoma<sup>10</sup>, which, since June 2006, has been generating high-resolution 3-D reflectivity mosaic grids (31 vertical levels) and a suite of severe weather and QPE products in real-time for the conterminous United States at a 1-km horizontal resolution and 2.5-min update cycle. The heights in the reflectivity mosaic grid are: 0.5, 0.75, 1, 1.25, 1.5, 1.75, 2, 2.25, 2.5, 2.75, 3, 3.5, 4,

---

<sup>8</sup> For details, visit [http://www.roc.noaa.gov/WSR88D/PublicDocs/DualPol/tin\\_10-23dual\\_pol88d.pdf](http://www.roc.noaa.gov/WSR88D/PublicDocs/DualPol/tin_10-23dual_pol88d.pdf).

<sup>9</sup> Visit <http://www.nws.noaa.gov/tg/radfiles.html>.

<sup>10</sup> Visit <http://nmq.ou.edu>.

4.5, 5, 5.5, 6, 6.5, 7, 7.5, 8, 8.5, 9, 10, 11, 12, 13, 14, 15, 16, and 18 km Mean Sea Level. The products are provided in real time to end users ranging from government agencies, universities, research institutes, and the private sector, and have been used in various meteorological, aviation, and hydrological applications. Furthermore, a number of operational QPE products generated from different sensors (radar, gauge, satellite) and by human experts are ingested in the MRMS system, and the experimental products are evaluated against the operational products and the independent gauge observations in real time. No dual-polarization products are available yet, but several are under development at University of Oklahoma, the National Oceanic and Atmospheric Administration's (NOAA's) National Severe Storms Laboratory (NSSL), and elsewhere. The MRMS is in the process of being implemented at the National Centers for Environmental Prediction (NCEP) as a fully operational system and will be used there to help with incorporation of radar data into NWP models.

### 3.6 TERMINAL DOPPLER WEATHER RADAR

Terminal Doppler Weather Radar (TDWR) is a 5-cm wavelength Doppler weather radar system used primarily for the detection of hazardous microburst and wind shear conditions on and near selected major airports in the United States. TDWR has varying resolution:

- Short range (all moments): 150 m resolution out to 90 km
- Long range (only reflectivity): 150 m–135 km and 300 m from 135 km–460 km
- For products:
  - Short Range Doppler (velocity and spectrum width): 150 m–90 km
  - Short Range Reflectivity: 300 m–90 km
  - Long Range Reflectivity: 600 m–276 km

The scan patterns are designed to cover the volume of terminal airspace in several minutes, with a low-level ( $0.5^\circ$  elevation) scan every minute for surveillance. The radars are situated in locations to optimize scanning over airport terminal areas; 47 active radars are located across the United States and Puerto Rico (see figure 11). Funded by the FAA, TDWR was developed in the early 1990s to assist air traffic controllers by providing real-time wind shear detection and high-resolution precipitation information.



**Figure 11. TDWR locations**

The narrower beamwidth of these radars ( $0.5^\circ$ ) compared to NEXRAD allows for measurement of more fine-scale detail of storms. The systems are not polarized, and only reflectivity and radial velocity are available; the coverage is not designed for weather monitoring across the CONUS. The data are not generally made available to the public, but are instead input to microburst and wind-shear algorithms that are displayed at Terminal Radar Approach Controls (TRACONS) and Air Traffic Control Towers at the respective airports. However, because the radars were designed to scan over the terminal area, their data could be highly useful for tracking precipitation as part of a TAIWIN system. Reflectivities below  $-20$  dBZ are available through the data stream (subject to the minimum detectable signal, which is range dependent), but typically only those greater than  $0$  dBZ are shown on TDWR user displays.

TDWR products (see table 2) are available via Radar Product Central Collection Dissemination Service; a subset is provided via NOAAPORT. The products consist of base and algorithm-derived products and are intended for distribution in near real-time. The base products are provided at 150-m range resolution and 300-m range resolution for the long-range reflectivity product. Algorithm-derived products are provided at the same resolution as the corresponding NEXRAD products (see table 1)<sup>11</sup>.

<sup>11</sup> Visit [http://www.nws.noaa.gov/tg/pdf/noaaport\\_radar\\_products.pdf](http://www.nws.noaa.gov/tg/pdf/noaaport_radar_products.pdf).

**Table 2. TDWR products**

Reflectivity—0.6° long range, Base , 1.0°, and a third elevation
Velocity—0.6° long range, Base , 1.0°, and a third elevation
Composite Reflectivity
Echo Tops
VAD Wind Profile
VIL
Storm Tracking Information
Hail Index
Tornadic Vortex Signature
1-H Precipitation Total
Storm Total Precipitation
Mesocyclone

Product definitions are the same as for NEXRAD. All products are archived at the National Climatic Data Center. “Level II” type real-time reflectivity and velocity data are not publicly distributed, but are made available to the NWS to be viewed on an Advanced Weather Interactive Processing System. The microburst and wind-shear products are available to airport tower and TRACON facilities.

### 3.7 COMMERCIAL RADARS

In addition to weather radars operated by the NWS and FAA, a number of vendors design and manufacture weather radars that may be suitable as part of TAIWIN<sup>12</sup>.

Additionally, shorter-wavelength radars, sometimes referred to as “cloud radars,” are becoming more widely available commercially. These radars have wavelengths in the millimeter to centimeter range and different capabilities than the longer wavelength instruments. Research has been conducted to determine their utility for detecting non-precipitating clouds that may present an inflight icing hazard [9 and 10], but cloud radar products directly addressing icing are not yet available commercially.

However, these radars may be used to detect cloud layers, and commercial versions include limited outputs. For example, the Metek K-band 24 GHz Micro Rain Radar is a relatively new instrument on the market (see figure 12). This radar is vertically pointing (no scanning capabilities) with a range of 30 m–6 km above the surface. The Micro Rain Radar MRR-2

---

<sup>12</sup> Lists of current radar vendors are available at <http://www.nws.noaa.gov/im/more.htm> and at <http://www.nwas.org/committees/rs/radar.html>. Most of these are C- and X-band and are used for weather surveillance and warning.

measures profiles of reflectivity and Doppler spectra. Derived products include drop size distributions, rain rates, liquid water contents, and path-integrated attenuation, though the accuracy of these products has not been verified. From time-height displays, the user can determine the height and location of multiple melting layers, or “bright bands.” Figure 13 is an example of a reflectivity time-height cross section from the Metek MRR-2 radar showing the bright band region (higher reflectivity; see scale at bottom right) at ~665–875 m AGL from 18:30–20:30, then dropping to below ~300 m.

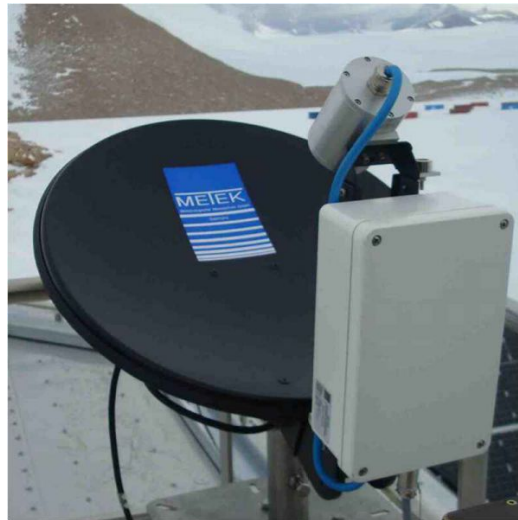


**Figure 12. The Metek K-band MRR-2 radar**

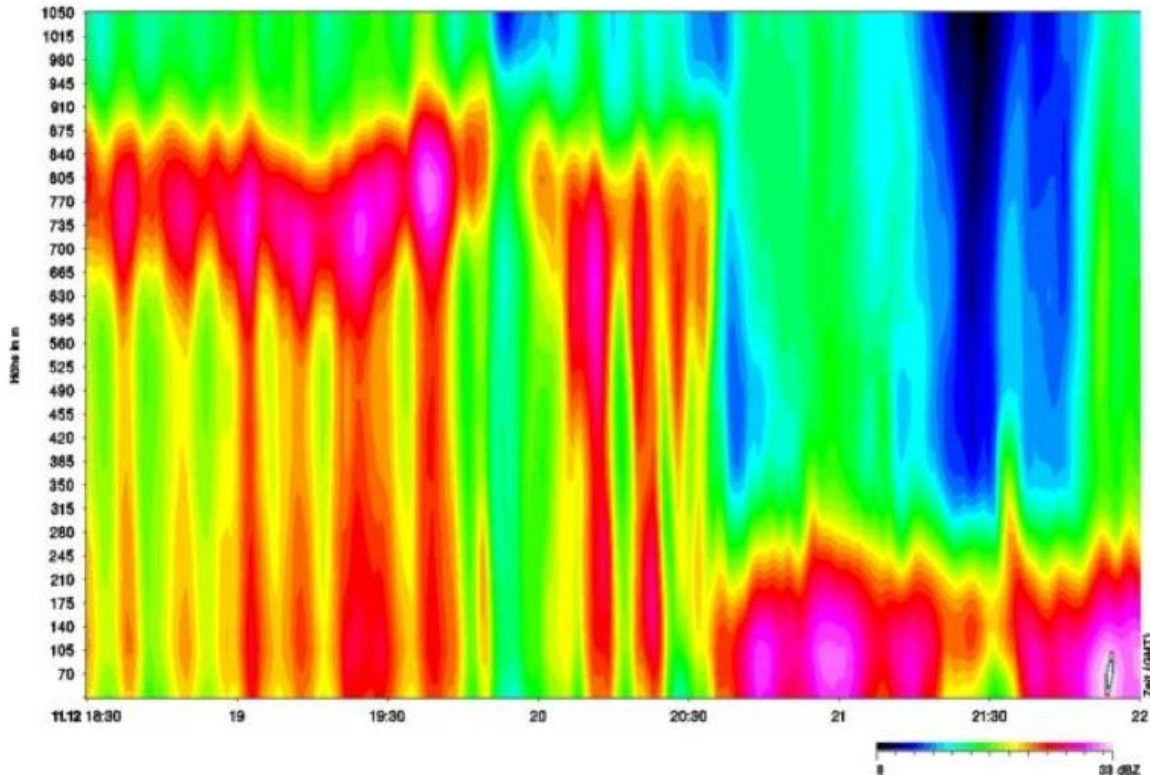


**Figure 13. Reflectivity time-height cross section from the Metek MRR-2 radar**

### 3.8 MICROWAVE RADIOMETERS

Though radars both transmit and receive radiation, radiometers are passive instruments that detect microwave radiation emitted or reflected by atmospheric components. By using various frequencies strongly emitted by water vapor, liquid, or ice, the total amounts of these in a narrow viewing window, or “beam,” can be retrieved [11]. Other frequencies emitted by various other gaseous atmospheric components at various levels of the atmosphere can be used to construct temperature and vapor profiles [12]. From these thermodynamic profiles and their trends in time, additional atmospheric parameters of interest to forecasters can be derived.

For example, Radiometrics Corporation manufactures several commercially available instruments (see figure 14) having 14–21 microwave channels (ranging from 22–59 GHz frequency), depending on the model capable of determining vertical temperature; water vapor and liquid water profiles; and other derived values. These instruments are capable of providing temperature and liquid profiles up to 10 km above the surface and total integrated liquid water and water vapor amounts. An infrared temperature sensor also gives information on cloud base temperature. The profiles are constructed using measurements from the instrument combined with radiative transfer retrieval models and, in the case of liquid profiles, a neural-net technique. Limited verification has been performed and, therefore, the accuracy of the profiles is not well established.



**Figure 14. A Radiometrics model MP-3000A profiling radiometer**

Numerous studies have described detection of inflight icing conditions using microwave radiometers, including those in references 13 and 14. These have shown good correlations of PIREPs of icing with high liquid water paths.

### 3.9 SATELLITE PRODUCTS

The Geostationary Operational Environmental Satellites (GOES) are in fixed orbits at 35,800 km (22,300 miles) above the earth's surface. Because they orbit the earth at its rotation speed, they are able to continuously monitor the same areas. The GOES-East (at 74.38° west longitude) and GOES-West (at 135.23° longitude) cover the CONUS; the seam line between the two is at approximately 100° longitude. The GOES imager has five channels spanning visible through long-wavelength infrared (see table 3) to image cloud extent and measure brightness temperatures<sup>13</sup> of cloud tops, the earth's surface, and various levels of the atmosphere. Data from the wavelengths are combined by algorithms to produce profiles of temperature and moisture and to derive cloud properties.

---

<sup>13</sup> Brightness temperature is the temperature a black body in thermal equilibrium with its surroundings would have to be to duplicate the observed intensity of a grey body object at a given frequency.

**Table 3. Current GOES imager instrument characteristics**

Channel Number	1 Visible	2 Shortwave IR	3 Moisture	4 IR 1	5 IR 2	6 IR 3
GOES 8-11 Wavelength ( $\mu\text{m}$ )	0.55 - 0.75	3.9	6.7	10.7	12	N/A
GOES 12-N Wavelength ( $\mu\text{m}$ )	0.55 - 0.75	3.9	6.5	10.7	N/A	13.3
Instantaneous Geographic Field of View at Nadir	1 km	4 km	8 km	4 km	4 km	4 km
Use	Cloud and surface features	Emitted and reflected IR for cloud and surface feature identification	Moist and dry areas at selected altitudes	Emitted IR for cloud and surface feature ID	CO <sub>2</sub> emissions	Replaces channel 5; broader response function

The various wavelengths have different penetration distances into clouds, but nominally they only measure conditions within approximately the first 100 m into the cloud. Visible wavelengths are used to determine where clouds are horizontally; the brightness of the visible signal may be used to infer particle type, such as ice crystals or water drops. Infrared wavelengths are used to derive the cloud top temperature. Horizontal resolution is ~1 km for visible wavelengths and ~4 km for infrared.

The GOES also carries a sounder that provides vertical profiles of temperature and moisture; different GOES versions have slightly different channels. For example, GOES-8 has eighteen thermal infrared channels plus a low-resolution visible channel. Table 4 lists typical wavelengths and their uses.

**Table 4. Current GOES sounder channels**

Channel	Wavelength ( $\mu\text{m}$ )	Purpose
Longwave		
1	14.71	Stratosphere temperature
2	14.37	Tropopause temperature
3	14.06	Upper-level temperature
4	13.96	Midlevel temperature
5	13.37	Low-level temperature
Window		
6	12.66	Total precipitable water
7	12.02	Surface temperature, moisture
8	11.03	Surface temperature
Ozone		
9	9.71	Total ozone
Water vapor		
10	7.43	Low-level moisture
11	7.02	Midlevel moisture
12	6.51	Upper-level moisture
Shortwave		
13	4.57	Low-level temperature
14	4.52	Midlevel temperature
15	4.45	Upper-level temperature
Nitrogen		
16	4.13	Boundary-layer temperature
Window		
17	3.98	Surface temperature
18	3.74	Surface temp., moisture
Visible	0.94	Cloud

Vertical temperature profiles are produced at forty pressure levels from 1000 to 0.1 mb using a physical retrieval method combined with a reasonable first-guess profile. Moisture is also profiled at the same vertical levels as temperature up to 300 mb. These profiles are valid only in clear or partly-clear fields of view. Layer composites are also available, as are sounder-derived images, such as land-sea temperature, lifted index, total column precipitable water vapor, and a cloud product, which shows the cloud top pressure over the viewed region. These products are available hourly.

The NASA Langley Research Center (LaRC) has developed a suite of products designed for aviation weather hazard identification based on GOES channels combined with surface data and NWP model outputs. An excellent summary of the motivation for the product development, their physical principles, and intended use is provided in reference 15. The algorithms rely on assumptions of hydrometeor size distributions and concentrations and their radiative properties to develop the products. Those most relevant to inflight icing diagnosis are listed in table 5.

**Table 5. NASA LaRC icing-related GOES products**

Product	Description
Effective Cloud Temperature	Estimate of cloud top temperature
Cloud Top Height	Height of cloud top
Optical Depth	In terms of $\tau$ , the extinction coefficient at visible wavelength. $\tau = 1$ means cloud is opaque to that wavelength.
Cloud Phase	Particle phase at cloud top (or surface conditions) categorized as snow/ice at surface, no/bad data, no cloud retrieval, clear, weak ice cloud, ice cloud, weak liquid cloud, liquid cloud $T < 273K$ , liquid cloud $T > 273K$ .
Effective Water Drop Radius	Calculated where LWP $> 0$ ; none or unknown elsewhere. Technically, the third moment of the water drop distribution divided by the second. Calculation is done via radiative transfer calculations based on an assumed water drop size distribution.
Effective Ice Particle Diameter	Calculated where IWP $> 0$ ; none or unknown elsewhere. Calculation is done via radiative transfer calculations based on an assumed ice particle size distribution.
LWP	Total columnar liquid water in $g\ m^{-2}$ calculated where Cloud Phase product indicates liquid
IWP	Total columnar ice in $g\ m^{-2}$ calculated where Cloud Phase product indicates ice
Icing Index	Nine levels including null based on cloud top temperature, $r_{eff}$ and LWP

LWP = liquid water path; IWP = ice water path;  $r_{eff}$  = cloud droplet effective radii

The icing product is described in reference 16, and other products are described in references 17–19. Images of the gridded products in JPEG format, or the data in Network Common Data Format (NetCDF), are available on the NASA Langley Cloud and Radiation Research Web page<sup>14</sup> and are generated from pixel-level data with 24-hour delay. Some of the

<sup>14</sup> The website, which also includes an extensive reference section, is found at <http://www-pm.larc.nasa.gov/>.

cloud product images (JPEG) and NetCDF are available in near-real time. Figure 15(a) shows pseudocolor cloud top temperature images; Figures 15(b–h) show cloud and icing parameters at 1545 UTC on March 15, 2004 [16].

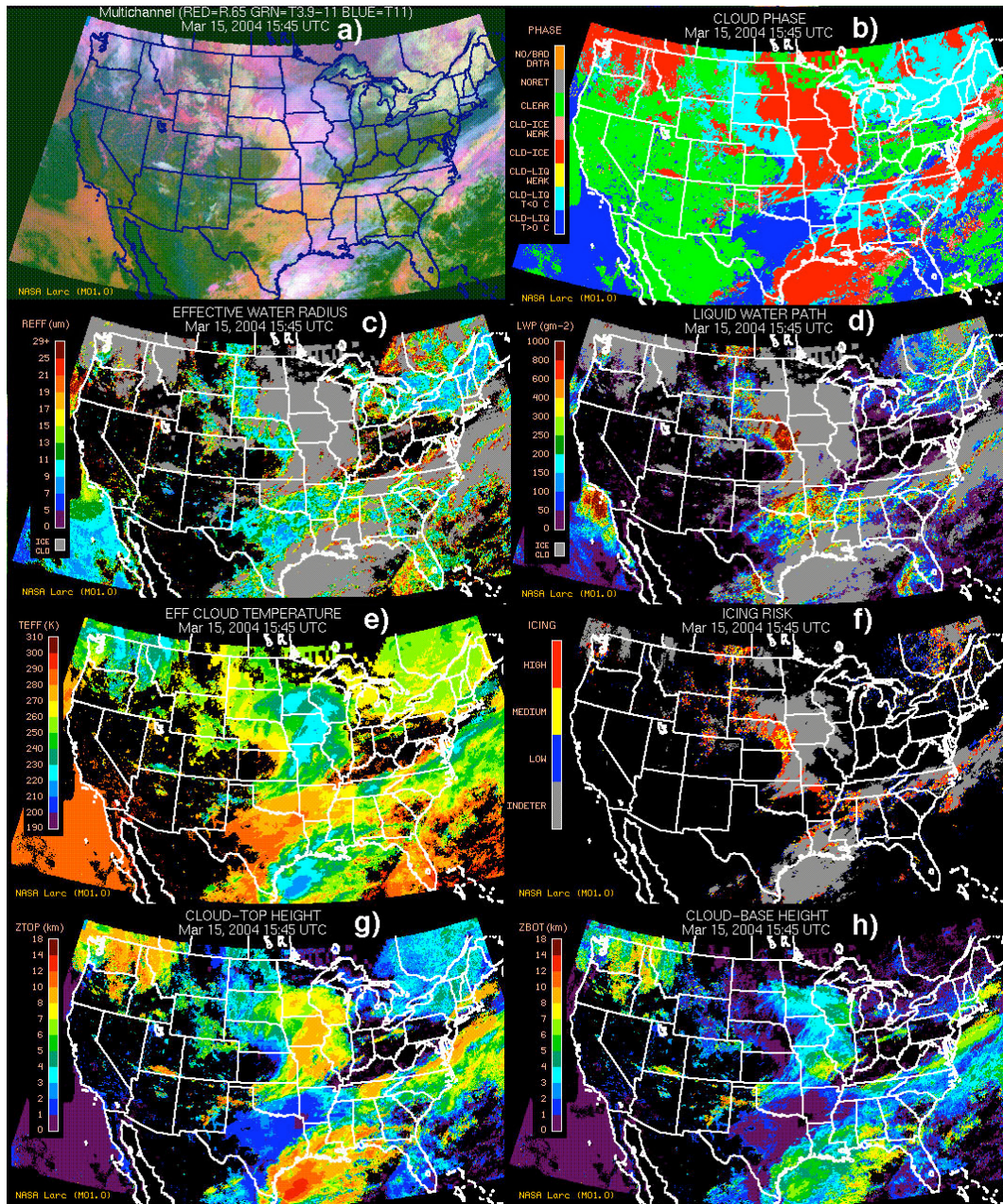


**Figure 15. Merged GOES (east and west)**

The products have been verified to varying degrees. In one study, the cloud phase product showed a combination of ice- and liquid-phase conditions in two cases in which icing conditions were observed by an aircraft [20]. In a third case from this study, in which aircraft measurements indicated ice-phase particles exclusively, the satellite retrieval was for ice. Retrieved  $r_{\text{eff}}$  were compared to measurements from a research aircraft and it was found that, though absolute values

were not in good agreement, the satellite retrievals showed some skill in estimating drop size at cloud top and may be useful for evaluation of large-drop regions [21]. The products on their own showed only poor-to-moderate skill in diagnosing icing, perhaps because of the two-dimensional nature of some of the products verified [22]. Issues with multilayered clouds were demonstrated, noting difficulties that the GOES Derived Cloud Products (GDGP) had with transition zones (edge effects) and changes in solar zenith angle while discussing the potential integration of GDGPs into the Current Icing Product (CIP) [23]. However, the advanced satellite products could help with icing diagnoses at high spatial resolution and could allow for more accurate icing diagnoses in areas where surface data are sparse (e.g., over oceans and Alaska).

The Polar Orbiting Environmental Satellite (POES) system provides daily global coverage by making nearly polar orbits 14 times per day approximately 520 miles above the earth's surface. Though the data are detailed and are used for weather monitoring, the utility is limited for real-time weather detection or forecasting because there are only two complete views at any given location per day over most of the mid-latitudes. In polar regions, the coverage is more frequent. The National Center for Atmospheric Research (NCAR) is currently examining the use of POES data for icing diagnosis in Alaska.

POES instruments include the Advanced Very High Resolution Radiometer (AVHRR) instrument and the Advanced Television Infrared Observation Satellites Operational Vertical Sounder (ATOVS) suite. The AVHRR and ATOVS provide visible, infrared, and microwave data used for a variety of applications, such as cloud and precipitation monitoring, determination of surface properties, and humidity profiles.

Other polar-orbiting systems exist that may provide limited but important information. The Nimbus 7 Scanning Multichannel Microwave Radiometer data were used to assess cloud liquid water content and precipitation characteristics of clouds over the Atlantic Ocean [24]. Their retrieval method was valid only over the ocean where estimates of emitted radiation could easily be made over the uniform surface. Methods were applied to develop a climatology of icing cloud characteristics over the north Atlantic [25]. The technique was extended to work over land surfaces, using the Advanced Microwave Scanning Radiometer (AMSR)—EOS [26]. Unfortunately, the AMSR is no longer available. The AVHRR satellite sensor data were used to estimate cloud particle phase for a variety of cloud types [27]. These techniques have the usual limitations of polar-orbiting satellites in that they have discontinuous views of specific locations; however, they may provide useful occasional clues regarding the structure of clouds.

CloudSat is part of the A-Train [28], a group of polar-orbiting remote sensing instruments launched to provide detailed views of clouds and the atmosphere. Note that it is an orbiting rather than stationary satellite; therefore, it provides information in a swath as it orbits and scans the earth perpendicular to its path. It carries a Cloud Profiling Radar (CPR, 94 GHz), which provides a vertical reflectivity profile of cloudy areas (see figure 16) without any information about the cloud phase. With its -28 dBZ minimum detectable signal, the CPR is able to detect most clouds, except those that are very thin or those that are made up of particles too small for the radar to detect well. It provides reflectivity data every 240 m from the surface to 30 km along the nadir

track. Derived products, such as hydrometeor type, precipitation rate, and visibility, are not available.

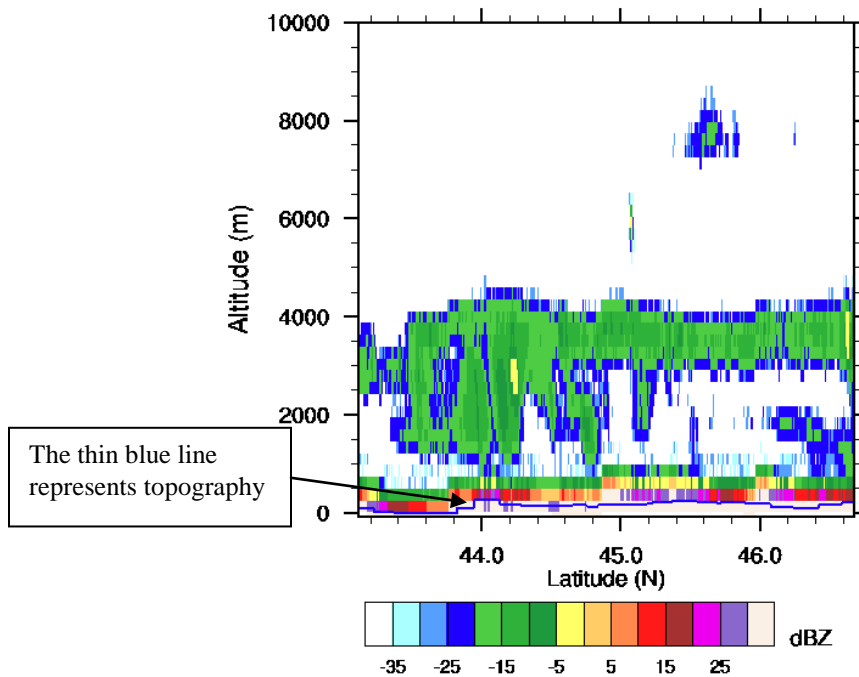


**Figure 16. CloudSat radar reflectivity cross-section from 2028–2029 UTC on November 5, 2006 [29]**

Though CloudSat provides highly detailed reflectivity profiles along its track, that track has limited coverage; data for any specific terminal area are not routinely available. However, when available, it has potential for providing detail on cloud cover and information on cloud structure. Data could also be used to verify other diagnoses and forecasts<sup>15</sup>.

### 3.10 THE GLOBAL AIRCRAFT METEOROLOGICAL DATA RELAY AND THE AIRCRAFT COMMUNICATIONS AND REPORTING SYSTEM

The global Aircraft Meteorological Data Relay (AMDAR) program was initiated by the World Meteorological Organization (WMO) and its members, in cooperation with aviation partners, and has led to the development of the AMDAR observing system. This system uses both new and existing aircraft onboard sensors, computers, and communications systems to collect, process, format, and transmit meteorological data to ground stations via satellite or radio links. Once received on the ground, the data are relayed to National Meteorological and Hydrological Services where it is processed, quality controlled, and transmitted on the WMO Global Telecommunications System. AMDAR produces over 300,000 high-quality observations of air

---

<sup>15</sup> Orbit patterns are available on the web (e.g., <http://www.osdpd.noaa.gov/ml/ppp/navpage.html>).

temperature, wind speed, and direction per day, together with the required positional and temporal information and with an increasing number of humidity and turbulence measurements.

Vertical profiles of AMDAR data are derived during ascent or descent at specified heights; en-route data are delivered periodically as the aircraft flies at cruise altitudes. The next addition to AMDAR will likely be improved turbulence data using the NCAR in situ turbulence algorithm [30], which derives atmospheric eddy dissipation rate from onboard inertial navigation system measurements. Icing is not currently transmitted.

In the 1990s, the FAA, Delta Airlines, and NCAR collaborated to send ice detector data from Delta Airlines Boeing 777 aircraft through the Aircraft Communications and Reporting System (ACARS). This demonstrated feasibility of using ACARS for icing data transmission; however, because air carriers spend most of their time at cruise altitudes above clouds with icing potential, the usefulness of using air carriers in cruise for ice detection is questionable. Deployment of ACARS on commuter-type aircraft that fly at lower altitudes would be more helpful; if more of the larger air carriers adopted the system, additional vertical soundings as planes ascended and descended in the terminal area would be useful.

### 3.11 TROPOSPHERIC AIRBORNE METEOROLOGICAL DATA REPORTING

The Tropospheric Airborne Meteorological Data Reporting (TAMDAR) system monitors weather encountered by aircraft during flight and transmits the information via a global satellite network in real time to a central ground-based receiving station [31]. TAMDAR was developed and is operated by a private company, AirDat, and is currently deployed only in the United States. Transmitted data related to icing conditions include presence of icing, temperature, and humidity. The data reports are automated and are independent of an airplane's avionics and communications systems. TAMDAR has been in continuous operation on regional airliners since late 2004.

Ice on the aircraft is detected by an optical sensor whose beam is occulted by accreted ice. TAMDAR is equipped with two independent infrared emitter/detector pairs mounted in a leading-edge recess to detect ice accretion. Each pair is mounted so that their beams will be blocked if at least 0.5 mm of ice collects on the leading-edge surface. Mounted within the aerodynamic section of the probe are internal heaters that melt the ice, after which the measurement cycle repeats. The heaters remain powered for at least 1 minute. The large electrical current flow to the probe affects the other measurements, so all data are flagged during deicing. The deicing cycle repeats if more icing is encountered. Comparison of sensor output with liquid water content data from a research aircraft implied good performance of the sensor, including ice detection and null detection [32]. Comparison of CIP output with and without TAMDAR positive icing data (negative reports were not included) showed little improvement of the automated product with these high-resolution, more frequent reports. However, this may not have been a fair test: CIP already had demonstrated high skill at finding icing conditions hourly for 20-km x 20-km x 1000-ft volumes. For an icing diagnosis with higher temporal and spatial resolution, these reports may be expected to have greater influence, especially if null reports are used to decrease probability and severity values.

One drawback to TAMDAR is that the data are not freely available to the public. Access to the data is provided only by a paid subscription service with AirDat. In the past, NWS subscribed to TAMDAR reports, which were used by forecasters and ingested into NWP models; however, this was discontinued in 2011 as a cost-savings measure.

### 3.12 COMBINED REMOTE SENSORS

It is reasonable to expect that combinations of sensors could provide a superior diagnosis of inflight icing conditions. A six-channel microwave radiometer was used to obtain continuous measurements of temperature, water vapor profiles, and liquid water paths. A radio acoustic sounding system (RASS) was used to obtain high-resolution profiles in the lowest 1500 m and wind profilers to assess icing conditions in a winter case study [33]. They concluded that a combination of measurements was needed to truly represent the icing environment. A dual-channel microwave radiometer, RASS, rawinsondes, wind profilers, a lidar ceilometer, and infrared satellite imagery were used to determine cloud altitudes and assign liquid water contents [34]. This was extended to a more general solution of moisture profiling (vapor and liquid) in a cloudy atmosphere [35].

The NASA Icing Remote Sensing System (NIRSS) [36] built upon these ideas and added additional capabilities for monitoring and diagnosis of remote icing. The NIRSS deploys a multichannel radiometer, a lidar ceilometer, and a vertically pointing radar (initially K-band, more recently X-band) to sense clouds above the instruments and determine their potential for icing conditions. The NIRSS has been demonstrated to have skill in diagnosing icing conditions aloft [37–39]. Future upgrades include a scanning capability for the radiometer; FZRN and FZDZ detection; and improved cloud, liquid water, and icing profiling logic.

These combined remote sensor techniques are not yet operational but are included here because they have near-term potential for remote icing diagnosis and are good candidates for future development under TAIWIN.

## 4. NWP MODELS

A description of the current state of NWP models is beyond the scope of this document. This section will focus on the operationally available NWP models most appropriate for TAIWIN. These NWP models are run at government agencies, meet reliability standards (for issue times), and have usually been subjected to a rigorous approval process for accuracy (in the forecast output). Various NWP models are also available from private weather vendors; these are not included in this discussion because they generally are not openly available and have not always been routinely verified.

### 4.1 NCEP OPERATIONAL MODELS

The currently used operational NWP models are the North American Mesoscale Forecast System (NAM), the Weather Research and Forecast (WRF), and the Global Forecast System (GFS). The WRF has several operational versions; the one relevant to this forecast problem is known as the

Rapid Refresh (RAP). Table 6 shows available icing-relevant parameters for the RAP, NAM, and GFS.

**Table 6. NCEP model output relevant to diagnosing icing conditions**

	RAP	NAM	GFS
Resolution	13 km horizontally, 50 vertical layers.	12 km horizontally, 60 vertical layers. Also a CONUS 4 km nest and Alaska 6 km nest	Graphical output for a 70 km grid, every 3 hours to 384 hours. Also a 27-km gridded file to 192 hours. 64 vertical layers.
Run	Hourly, output 1 hour increments to 18 hours	00Z, 06Z, 12Z, 18Z. Output to 84 hours, at 3 hour increments	00Z, 06Z, 12Z, 18Z. See above for output times.
Temperature	At grid points and also at 2 m AGL	At grid points and also at 0–30 mb AGL	At grid points
Moisture	Specific humidity, RH at grid levels points and also at 2 m AGL	RH at grid points and also at 0–30 mb AGL	RH at grid points
Total precipitation (various accumulation periods)	yes	yes	yes
Convective precipitation	yes	yes	no
Cloud water mixing ratio	yes	yes	no
Rain water mixing ratio	yes	no	no
Ice mixing ratio	yes	yes	no
Snow water mixing ratio	yes	no	no
Graupel mixing ratio	yes	no	no
Ice particle number concentration	no	no	no
Snow accumulation	Uses a 10:1 liquid/snowpack ratio from accumulated snow water equivalent	no	no
Categorical precipitation	Yes/no for snow, ice pellets, FZRN, rain – experimental only!	Yes/no for snow, ice pellets, FZRN, rain	no

RH = relative humidity

Note that the mixing ratios refer to the mass of the given substance to mass of air, usually given in grams/kilograms in model output.

The operational version of RAP includes high-frequency (every hour) three-dimensional objective analyses over all of North America, assimilating the following types of observations [40]:

- Commercial aircraft (including moisture data from WVSS-II sensors)
- Radar and wind profiler products
  - Wind profiles (from available NOAA-operated 404 and 915 MHz)
  - VAD (velocity-azimuth display) winds from NWS WSR-88D radars
  - RASS
- Rawinsondes and special dropwindsondes
- Radar reflectivity (3D, from NSSL MRMS)
- Surface
  - Surface reporting stations and buoys (including cloud, visibility, current weather)
  - Mesonet (defer to RAP version 2)
- Satellite
  - AMSU-A/B satellite radiances
  - GOES satellite radiances (defer to RAP version 2)
  - GPS total precipitable water estimates
  - GOES cloud-top data (pressure and temperature)
  - GOES high-density visible and IR cloud drift winds
- Experimental
  - Lightning - defer to RAPv2 (used in ESRL RAP since Jan 2012)
  - Special wind-energy observations - defer to RAP version 2 (used in ESRL RAP)

An online verification tool for RAP<sup>16</sup> includes 2-m temperature and dewpoint. The Mean Bias Errors in these two parameters over the CONUS are typically  $<1^{\circ}\text{C}$ <sup>17</sup>.

#### 4.2 NCEP EXPERIMENTAL ENSEMBLE FORECAST

The NCEP's Very Short Range Ensemble Forecast (VSREF) provides probabilistic forecast information. The VSREF Aviation Project, a subset of the NCEP VSREF system, seeks to further improve the utility of VSREF products by applying ensemble techniques to aviation weather forecasts. Though these are considered “experimental” by NCEP (i.e., the code is not frozen and is run on a time-available basis), the output is available and could be used in TAIWIN.

An ensemble forecast is composed of a set of model outputs for the same time, which are referred to as “ensemble members.” The ensemble members can be from the same model using different initial or boundary conditions or physics schemes; from different models; or from a combination of the above. Time-lagging can also be done, in which model outputs for the same time from runs with varying start times are combined. The outputs from the various ensemble members are used in statistical computations to create probabilistic forecast information such as an ensemble mean, spread (typically expressed as standard deviation), and probability of occurrence. The VSREF uses 21 members and is generated every 3 hours with forecasts to 84 hours.

The icing environment depends primarily on temperature, humidity, and cloud water content at certain levels. Because the current ensemble members lack cloud water content, VSREF uses a T-RH (temperature-relative humidity) algorithm to predict icing. The forecasts are experimental and are issued for testing and feedback (see figures 17–19).

---

<sup>16</sup> Visit <http://rapidrefresh.noaa.gov/verify/Welcome.cgi>.

<sup>17</sup> Only total precipitation in a 24-hour period is verified on the website [http://ruc.noaa.gov/precipVerif/Welcome.cgi?dsKey=ruc\\_nssl\\_precip](http://ruc.noaa.gov/precipVerif/Welcome.cgi?dsKey=ruc_nssl_precip).

SREF: Probability of icing at FL180 00H FCST  
from 09z Jul 16 2012. Verified Time: 09z 07/16/2012

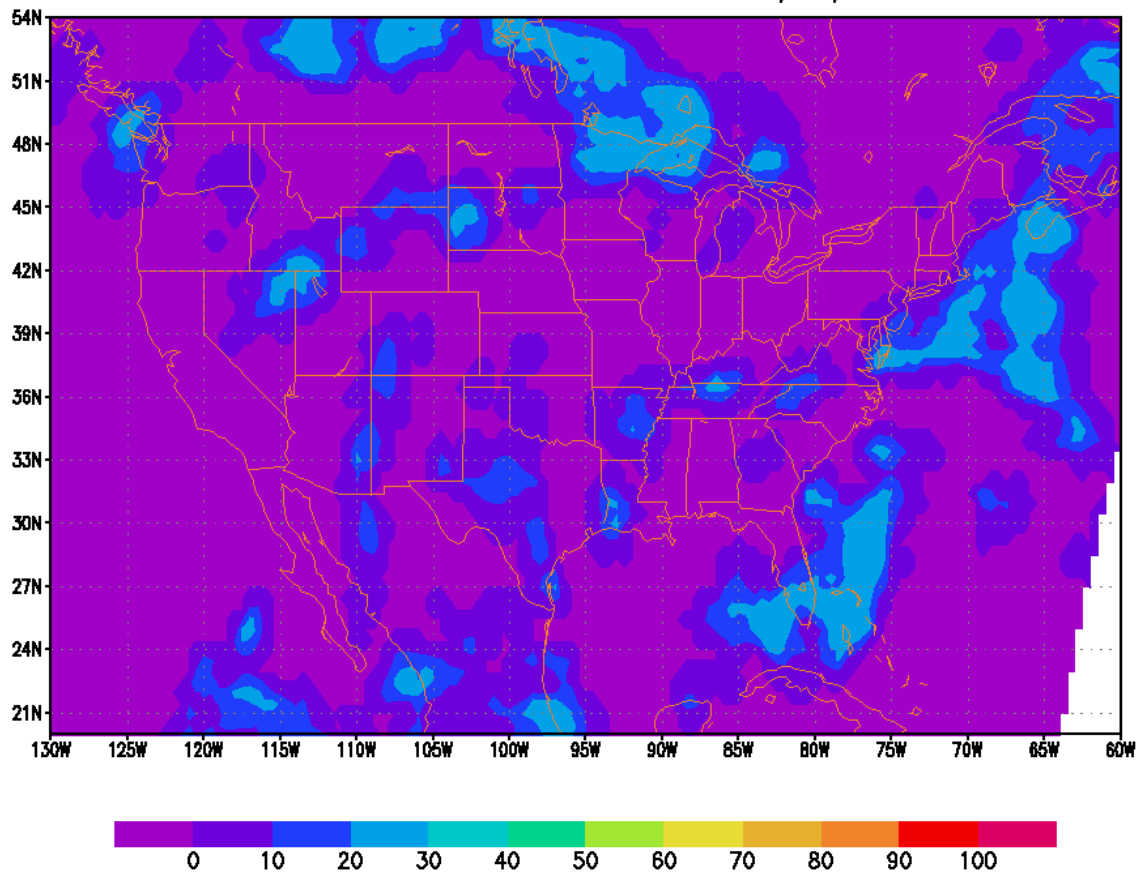


Figure 17. VSREF forecasts of icing at 18,000 ft for 1800 UTC—July 16, 2012<sup>18</sup>

<sup>18</sup> Current maps can be viewed at [http://www.emc.ncep.noaa.gov/mmb/wd20bz/SREF\\_aviation/web\\_site/html\\_212/icing.html](http://www.emc.ncep.noaa.gov/mmb/wd20bz/SREF_aviation/web_site/html_212/icing.html).

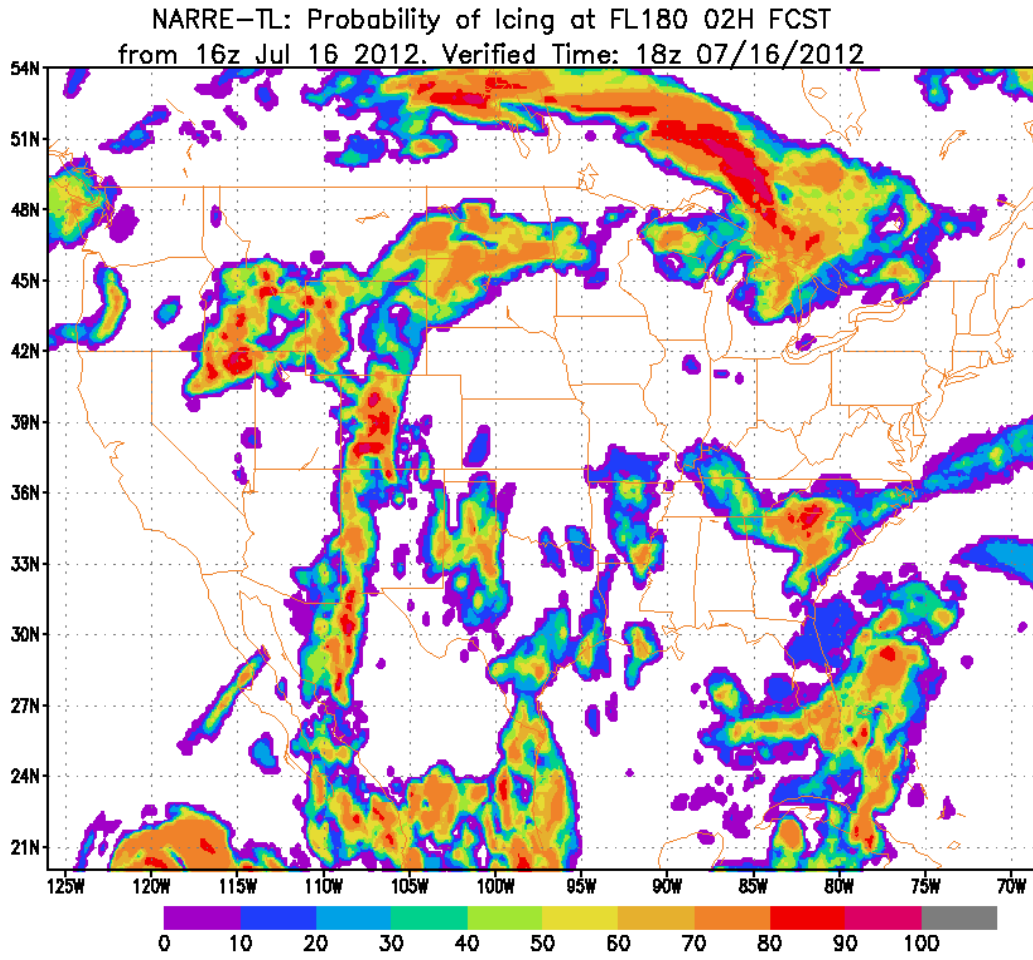
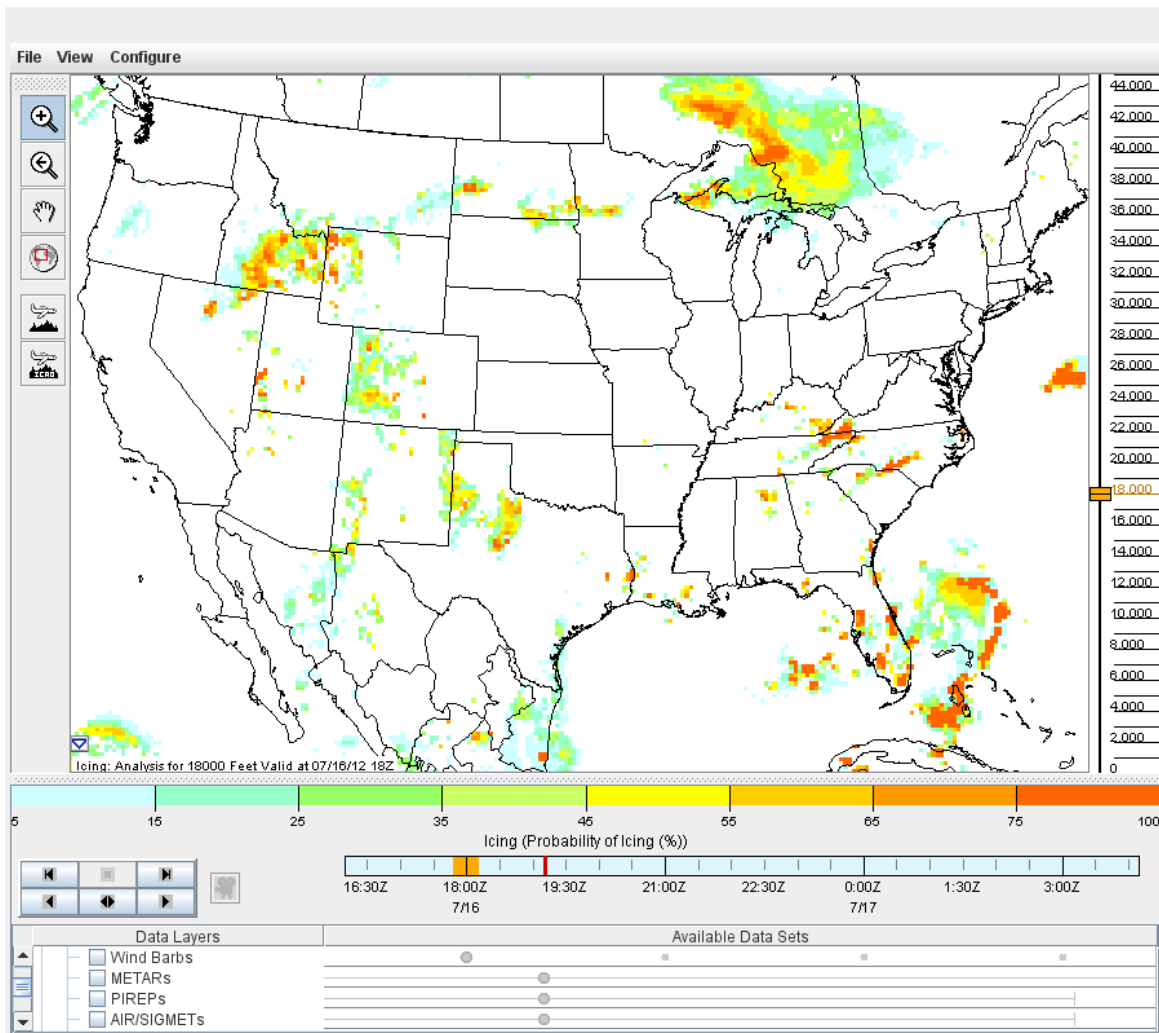


Figure 18. NARRE-TL forecasts of icing at 18,000 ft for 1800 UTC— July 16, 2012<sup>19</sup>

<sup>19</sup> Current maps can be viewed at [http://www.emc.ncep.noaa.gov/mmb/SREF\\_avia/FCST/NARRE/web\\_site/html/icing.html](http://www.emc.ncep.noaa.gov/mmb/SREF_avia/FCST/NARRE/web_site/html/icing.html).



**Figure 19. CIP analysis of forecast at 18,000 ft for 1800 UTC on July 16, 2012—from Aviation Digital Data Service flight path Java tool<sup>20</sup>**

The range of conditions for icing is temperature between  $-10^{\circ}\text{C}$ – $0^{\circ}\text{C}$  with relative humidity  $>70\%$ . Icing is computed at these flight levels (with approximate pressure levels):

- FL000: surface
- FL030: 3000 ft (900mb)
- FL060: 6000 ft (800mb)
- FL090: 9000 ft (725mb)
- FL120: 12,000 ft (650mb)
- FL150: 15,000 ft (575mb)
- FL180: 18,000 ft (500mb)
- FL240: 24,000 ft (400mb)

<sup>20</sup> Java tool available at <https://www.aviationweather.gov/adds/fptapplication/>.

At these levels and corresponding model grid points, if temperature and relative humidity both meet the icing criteria above, then the icing condition is “yes.” The probability calculation is rather simple. If  $M$  ensemble members out of all  $N$  members predict icing conditions at the same level and grid point, then the icing probability is  $M/N \times 100\%$ .

A new experimental icing probability product is also available over the CONUS using the North America Rapid Refresh Ensemble (NARRE) as the base model. The North America Rapid Refresh Ensemble Time Lagged (NARRE –TL) version is based on time-lagging of 6 RAP and 4 NAM operational runs. It covers CONUS at 13-km horizontal resolution, Alaska at 11-km horizontal resolution, and runs 24 cycles per day with hourly output of 12 forecast hours.

The NARRE-TL generates an ensemble for a given forecast time by combining the latest forecast with those issued earlier for the same forecast time. Usually, more recent forecasts are weighted more heavily than those issued earlier based on the assumption that more recent forecasts should be more accurate. The output provides a measure of the uncertainty of the forecast—for example, if all the forecasts for a given time are similar, this indicates high model certainty.

The NARRE output includes both en-route products (icing, turbulence, jet stream, convection, etc.) and terminal-area products (visibility, ceiling, fog, reflectivity, etc.). During the time-lagging, more recent runs are given higher weights, with which the ensemble mean, spread, and probability are computed. The icing algorithm and output products are the same as for the VSREF<sup>21</sup>.

The NARRE and VSREF icing forecasts are provided in terms of the probability of encountering icing conditions. They were analyzed using reliability plots for forecasts between April 28, 2011 and June 29, 2011 at 725 mb and 500 mb (see figure 20). The observed frequency of icing is plotted against the forecast frequency (e.g., for 725 mb, when icing was forecast at the 60% probability level, it was observed 38% [NARRE-TL] or 44% [VSREF] of the time). The “observations” are CIP diagnoses in this analysis. Even though this analysis was performed for conditions aloft (725 mb at 9000 ft and 500 mb at 18,000 ft), they show a similar trend of under-prediction at low frequency/probability and over-prediction at high frequency/probability. It is not known whether this trend exists near the surface.

---

<sup>21</sup> Visit [http://www.emc.ncep.noaa.gov/mmb/SREF\\_avia/FCST/NARRE/web\\_site/html/icing.html](http://www.emc.ncep.noaa.gov/mmb/SREF_avia/FCST/NARRE/web_site/html/icing.html).

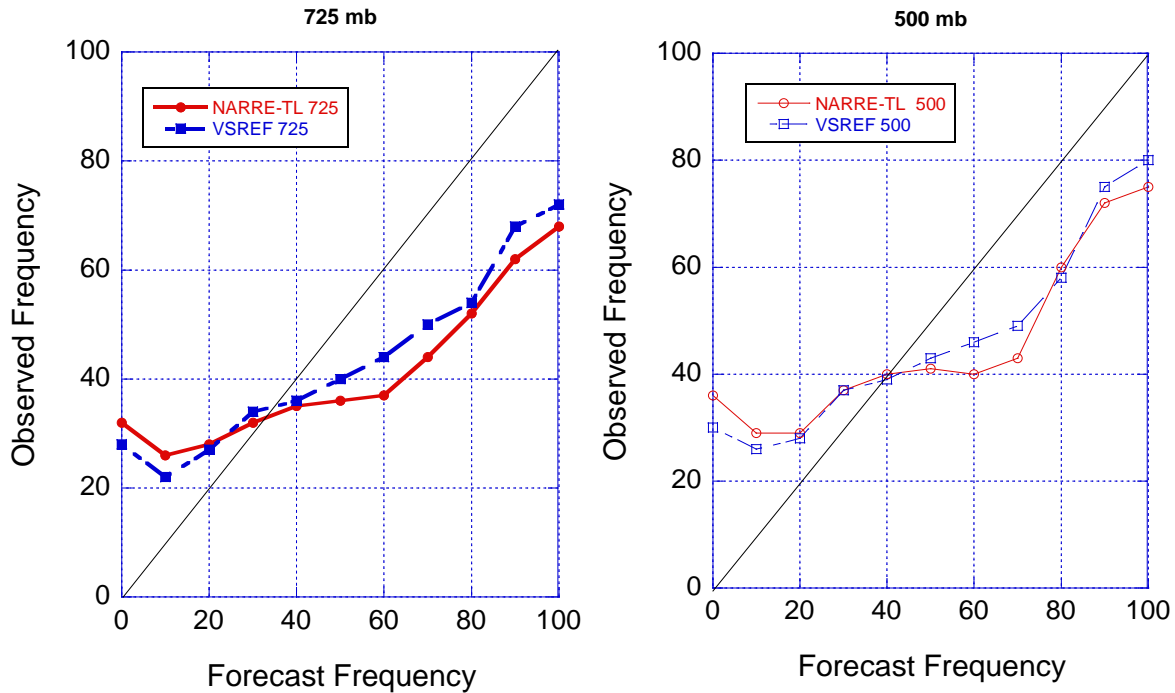


**Figure 20. Reliability plots for NARRE-TL and VSREF [41]**

## 5. ALGORITHMS

### 5.1 CIP AND FORECASTING ICING PRODUCTS

The CIP and Forecast Icing Products (FIPs) produce hourly diagnoses and forecasts (2-, 3-, 6-, 9-, and 12-hours) of expected inflight icing conditions across the CONUS with 20-km x 20-km x 1000-ft resolution. The CIP and FIP are run at the NWS's AWC and were developed at the NCAR under support of the FAA's Aviation Weather Research Program (AWRP). The CIP and FIP describe aircraft icing conditions in terms of expected severity, probability of encounter, and likelihood of supercooled large droplet (SLD) conditions. The severity estimation [23] is a broad-brush approach and meant to be guidance for all aircraft; it is roughly based on an accretion rate using combinations of assumed drop size and LWC [42]. Probability refers to the likelihood that icing of any severity will be encountered in any grid box. The SLD output is an uncalibrated scale from 0–1 describing the likelihood of encountering those conditions. Precipitation type is ingested from METAR information or NWP model output and is carried within the algorithm as an intermediate field to help assess the icing environment. It is not produced as an output of the algorithm and has not been verified, primarily because of a lack of observations aloft. The CIP combines the NWP model and observational datasets (from GOES, METARs, the National Lightning Detection Network, NEXRAD reflectivity, and PIREPs) to estimate where inflight icing conditions are likely and are not likely to occur. The algorithm uses fuzzy logic to accomplish this. The FIP is similar but, because it is a forecast, relies exclusively on NWP model fields as input. A full description of CIP is given in reference 43; FIP is described in reference 44.

Neither CIP nor FIP was designed to address the needs of ground icing (i.e., to provide guidance regarding precipitation amount or type). Similarly, they are probably not calibrated well for near-surface icing. The researchers used PIREPs of icing during development to develop and confirm fuzzy logic maps (e.g., for temperature and relative humidity) and to assess the quality of the product. There are relatively few PIREPs at low altitudes, presumably because that is a busy time for pilots flying approaches or departures in terminal areas. If weather conditions are poor, such as low ceilings and poor visibility (as there would be in most cases with icing conditions), the pilot is likely to have a heavy workload navigating the area and communicating with the Air Route Traffic Control Center or TRACON, and issuing a PIREP would only add to his workload.

One of the techniques used to assess quality is to compare forecasts with PIREPs of icing or no icing. If a PIREP of icing resides within a forecast icing area, or a PIREP of no-icing resides within a forecast no-icing area, a hit is recorded. Otherwise, a miss is recorded. Various thresholds of severity and probability may be used to define a forecast icing area and to sort the data. Simple probability of detection (POD) statistics for hits and misses can be formed:  $POD_{y,n} = \text{hit}/(\text{hit}+\text{miss})$ . Of course, one statistic does not tell the entire story: a  $POD_y$  ( $POD_n$ ) of 100% can be achieved either by forecasting icing everywhere all the time, or by forecasting no icing everywhere all the time. Calculating both  $POD_y$  and  $POD_n$  can reveal more about the forecast quality; however, because positive icing PIREPs tend to outnumber negative ones by at least a 10:1 ratio, knowledge of the absence of icing conditions is difficult to assess. The statistics shown in figure 21 reveal some information about CIP and FIP performance at low altitudes.  $POD_y$  for CIP and FIP are quite similar at all altitudes except the lowest; here  $POD_y$  for CIP is much greater than for FIP. This suggests that the additional observations (METARs, satellite, radar) incorporated by CIP improve its prediction of icing there. For  $POD_n$ , there is little difference; the additional information does not appear to significantly change the algorithms' ability to correctly forecast or diagnose non-icing conditions. In fact, FIP is slightly more successful in predicting non-icing conditions at most altitudes. This may imply that FIP produces smaller icing areas. Data in figure 21 are from winter 2005; FIP lead time is 6 hours,  $POD_y$  is for MOG icing, and the severity threshold is 0.10. Statistics were calculated at 3000-ft MSL intervals; each point on the graph is shown at the midpoint of the interval (e.g., 1500 ft, 4500 ft, etc.). The dashed lines show the estimated confidence intervals for their respective PODs.

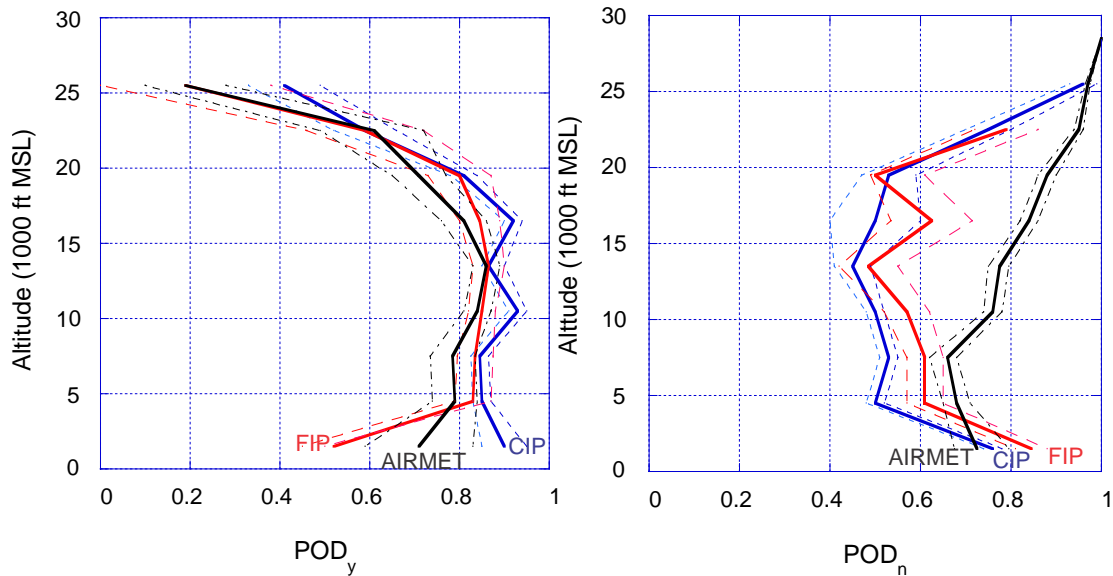


**Figure 21. Performance statistics for FIP, CIP, and AIRMETs as a function of altitude [45]**

## 5.2 LOWICE

LOWICE was created in response to a need for predictions of icing conditions at or near the surface for wind turbine icing [46]. It is intended to help the power industry react appropriately to short-term forecast surface icing conditions. LOWICE uses CIP concepts as a basis and adds estimates of supercooled liquid water content and ice accretion rate (see figure 22). An initial version of the algorithm is being run over Scandinavia using the Finnish Meteorological Institute version of the Local Area Prediction System (LAPS) analysis as its primary data source [47]. LAPS ingests data from the European Centre for Medium-Range Weather Forecasts NWP model, METARS, Meteosat-9 geostationary satellite, and a network of weather radars and other datasets to produce both two- and three-dimensional grids that LOWICE uses to assess near-surface icing conditions. The LOWICE output is hourly at a horizontal resolution of 3 km, with variable vertical spacing. A formal verification has not been completed, but comparison of LOWICE output with independent surface observations of cloud-base and tower-mounted probes, including ice detectors, showed good agreement [46].

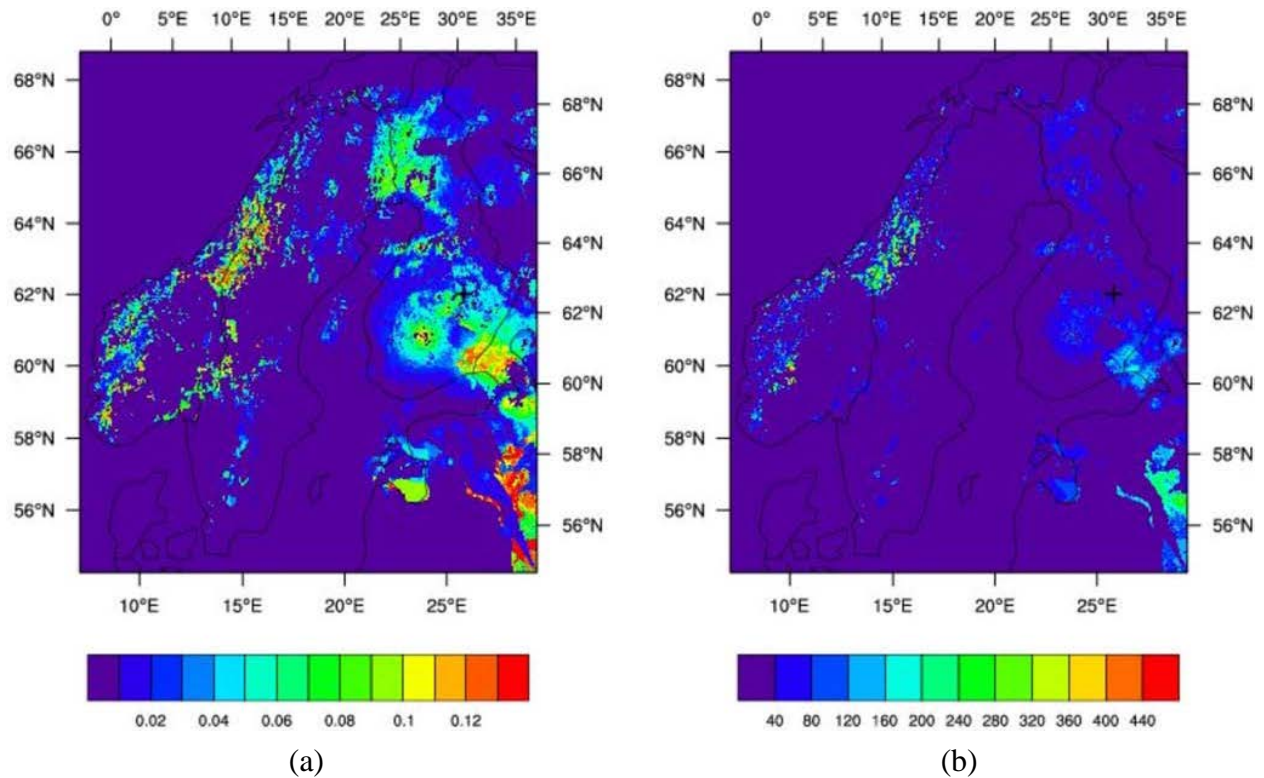


**Figure 22. Example plots of estimated (a) LWC ( $\text{g m}^{-3}$ ) and (b) icing rate ( $\text{kg m}^{-2} \text{h}^{-1}$ ) at 90 m AGL over the LOWICE Scandinavia domain [46]**

### 5.3 SYSTEM OF ICING GEOGRAPHIC IDENTIFICATION IN METEOROLOGY FOR AVIATION

The System of Icing Geographic Identification in Meteorology for Aviation (SIGMA) algorithm provides a real-time display of icing risk [48 and 49]. SIGMA uses a combination of data from an NWP model (ARPEGE, AROME, and ALADIN have been used), METEOSAT satellite imagery, and operational radar (Meteo France’s ARAMIS operational network plus other radars covering much of Europe). The radar data are collected every 15 minutes and have a horizontal resolution of 1 km, which forms the base map of SIGMA. Infrared images from METEOSAT with 4-km resolution are produced every 15 minutes. The observations, combined with the NWP model output, are used to determine cloudy areas (the surface temperature field from the NWP model is used to characterize the surface in the satellite imagery) and to infer temperatures at the tops of clouds. A ten-level icing index is derived from the model temperature and humidity fields at each cloudy grid point (see figure 23). The index is calibrated using the results of a climatological study of surface freezing precipitation over Europe. Upward vertical velocity is used to further refine the index. The radar reflectivity is processed into drizzle/cloud drops (low reflectivity), rain (moderate reflectivity), strong rain (high reflectivity), and null. The images are mapped to the model levels to show areas where there is greater risk for icing, as confirmed by the radar echo.

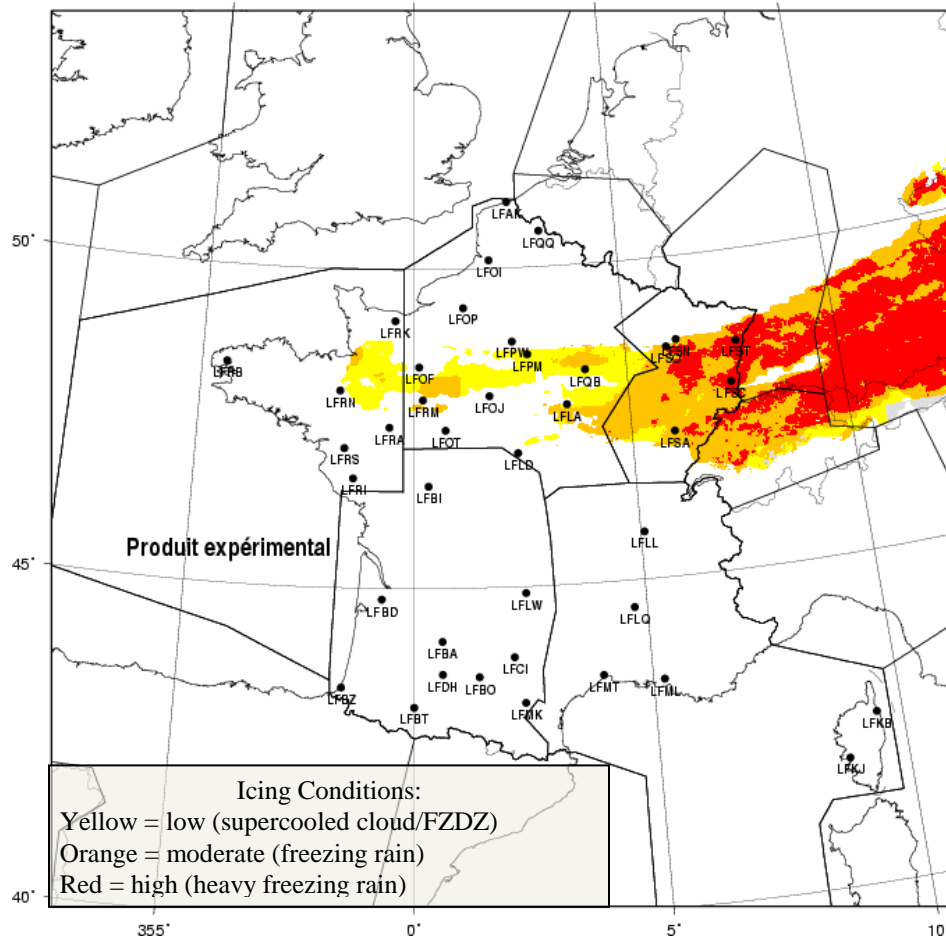


**Figure 23. SIGMA algorithm icing index output [49]**

Additional data, such as Doppler velocity, additional radar altitude scans, more satellite channels, and local-area NWP models, are available in some areas and have been added to SIGMA where they exist. These are mostly in terminal areas. Therefore, higher-resolution SIGMA outputs can be computed there.

A comparison between SIGMA and PIREPs of icing showed SIGMA had a 77% probability of correctly predicting icing (yes or no), and an 88% probability of predicting icing where a PIREP indicated it was present [49]. However, the false alarm rate was 48%. These results could be an artifact of the comparison method: a two-dimensional “footprint” of icing index was used rather than considering icing at the altitude of the PIREP. This meant that when the icing index at any level was positive, the entire column of the atmosphere was considered to include icing. A verification including altitude was also conducted and showed similar performance statistics for CIP and SIGMA when compared to PIREPs of icing [50]. A 3-D verification of SIGMA was performed, showing that for an algorithm threshold of 0.35/3.5 for CIP/SIGMA,  $POD_y$  was 0.76/0.74 and  $POD_n$  was 0.67/0.59 [51]. It is not surprising that the two algorithms have similar results because they use similar input datasets and methodologies.

## 5.4 ADVANCED DIAGNOSIS AND WARNING SYSTEM FOR AIRCRAFT ICING ENVIRONMENTS

The Advanced Diagnosis and Warning System for Aircraft Icing Environments (ADWICE) was developed for Europe through joint cooperation of the Institute for Atmospheric Physics at the German Aerospace Center (DLR), the German Weather Service (DWD), and the Institute for Meteorology and Climatology of the University of Hannover [52]. ADWICE combines data sources to identify icing conditions, beginning with the DWD’s Consortium for Small Scale Modeling—Europe (COSMO-EU NWP) model to derive a “first-guess” icing field by applying a variation of the original NCAR/RAP icing algorithm. This was completed by examining temperature and relative humidity profiles and applying thresholds to those values to determine the likelihood of icing conditions as appropriate for various meteorological regimes [53]. Four regimes are identified: general, unstable, warm stratus, and FZRN. At that point, observations are incorporated, including surface weather reports (SYNOPS and METARs) and radar reflectivity from the European radar network. The output consists of two icing fields, icing class (representing probability) and icing intensity, at a resolution of 7 km and selected pressure levels.

The DLR and NCAR collaborated on a comparison of ADWICE and FIP to learn more about the strengths and weaknesses of each system [54]. The European COSMO-EU model was executed on the eastern CONUS in winter 2009–2010 to produce input data for ADWICE. Only ADWICE model-based forecasts were used; therefore, no observational data were ingested. The FIP outputs matching ADWICE analysis times were used for a six-week comparison. For both algorithms, only forecasts of MOG icing severity were used; predicted icing at lower severity levels were treated as a prediction of no icing for this analysis. PIREPs were used as verification data (same MOG criterion).  $POD_y$  and  $POD_n$  were defined as in section 5.1, and the results are shown in figure 24.

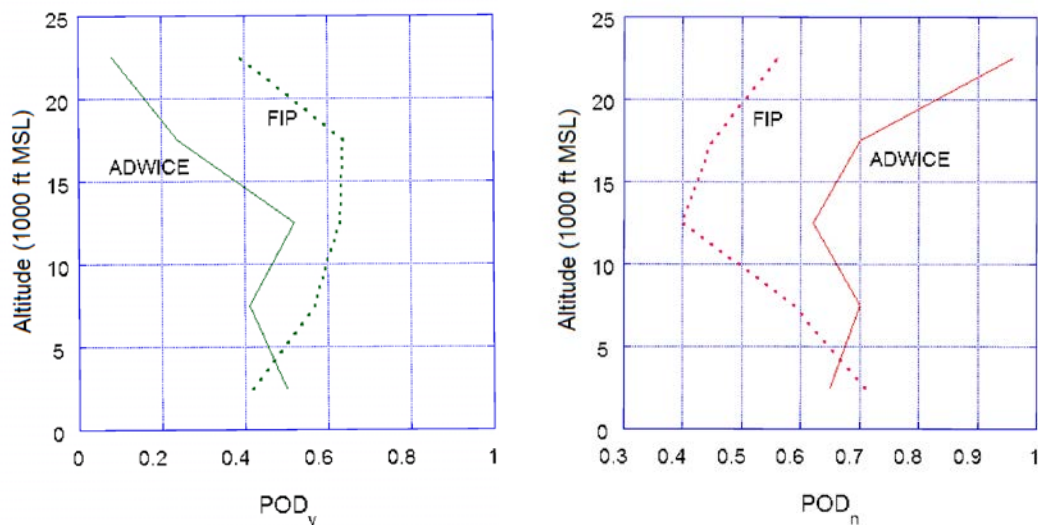


**Figure 24. Vertical distribution of  $POD_y$  and  $POD_n$  values for ADWICE and FIP [54]**

Throughout the altitude levels evaluated, FIP generally had higher  $POD_y$  and lower  $POD_n$  than ADWICE. Based on the  $POD_y$  and  $POD_n$  data, it was concluded that both ADWICE and FIP

slightly underforecast icing at low altitudes [54]. At the lowest level, 0–5000 ft (MSL, shown at the midpoint of 2500 ft on figure 24), the ADWICE POD<sub>y</sub> was slightly higher than that of FIP. This is either because of differences in the underlying NWP model (COSMO–EU vs. RUC) or in how the algorithms treat information in analyzing icing conditions.

## 5.5 GLOBAL ICING FORECAST PRODUCTS

The NWS’s AWC has the responsibility, as part of the World Area Forecast Center, Washington, to provide global weather forecasts of significant weather phenomena. Presently, the AWC produces High Level Significant Weather charts covering two thirds of the globe, which are issued four times per day. Recently, the AWC has accepted the responsibility for routinely providing a Mid-Level Significant Weather chart, between FL100 and FL450, for the North Atlantic Ocean Region. The Mid-Level chart’s low-altitude limit is FL100; therefore, they are not suitable for the terminal area.

## 6. DECISION SUPPORT SYSTEMS

### 6.1 WEATHER SUPPORT TO DEICING DECISION MAKING

The weather support to deicing decision making (WSDDM) system is a real-time decision support tool for mitigation of the impact of winter weather on aviation [55]. Developed by NCAR and the FAA, WSDDM uses data from WSR-88D radars and ASOS observations and additional mesonet sensor sites that use snow gauges and are strategically placed in and around the airport region within a 100-mile radius of the airport. These data are integrated into the WSDDM system, where past, current, and forecast data are displayed in real-time (see figure 25) to a variety of users, including airport operations managers, ground de-icing crews, ramp operations personnel, and runway plowing operations personnel. Radar data are updated every 5–6 minutes, whereas airport mesonet data are updated every minute. Winter weather trends are displayed graphically, and the nowcasting system TREC (Tracking Radar Echoes by Correlation) provides 30-minute predictions of radar reflectivity and liquid equivalent snowfall rates. Of special significance are the 1-minute mesonet updates of liquid equivalent snowfall rates, shown to be of particular importance in estimating the fluid holdover time of airplanes once de-icing and anti-icing fluids have been applied.

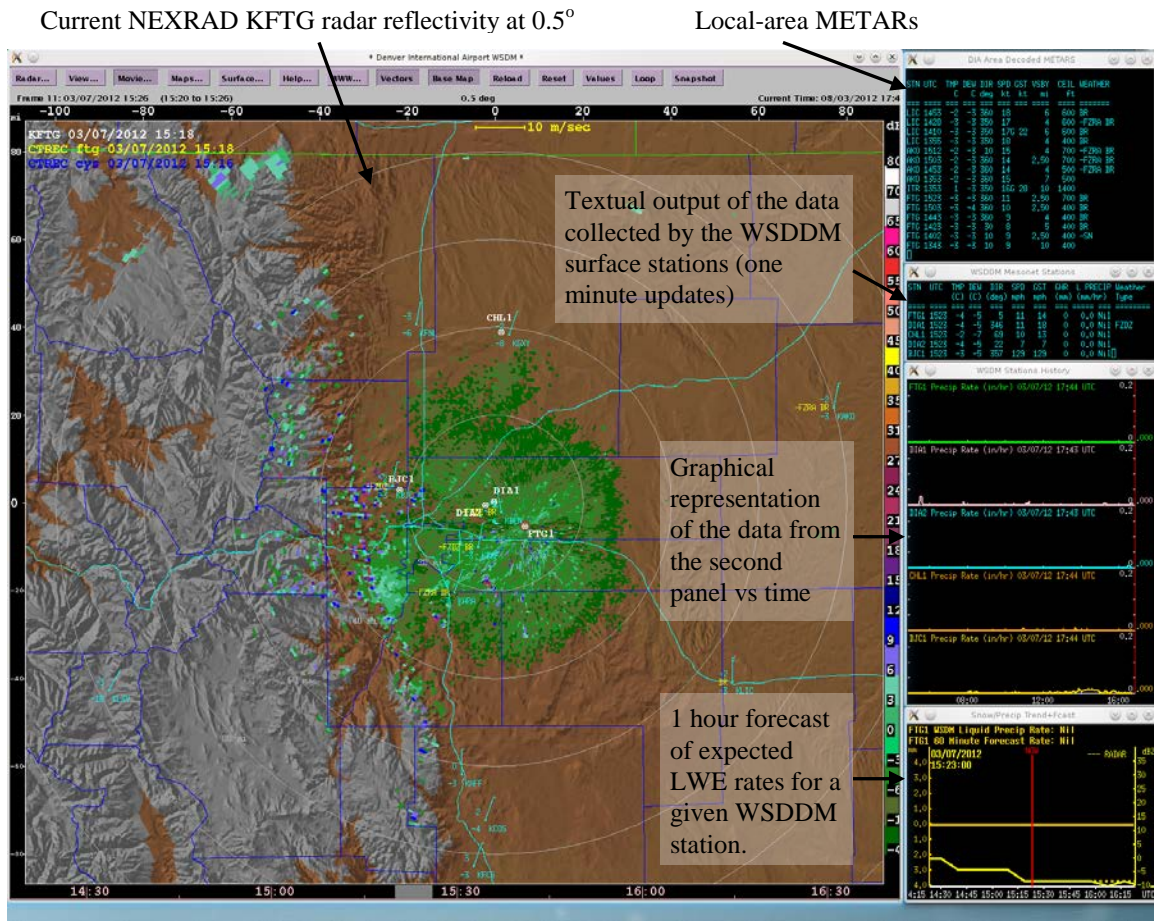


**Figure 25. The WSDDM real-time display for Denver International Airport**

WSDDM also uses the BFGoodrich ice detector sensor at its sites and uses a slightly modified algorithm to determine freezing precipitation accretion rates. The threshold frequency at which the system determines a freezing precipitation event is occurring was raised to 39,980 Hz (from ASOS's 39,972Hz) to more quickly catch the start of freezing precipitation events. The proposed ASOS FZDZ algorithm was also implemented in WSDDM, giving the system the capability to detect both FZRN and FZDZ. Freezing fog is not implemented in the system because the accretion rates from freezing fog can be similar to rates for FZDZ. Because FZDZ is considered more hazardous to aircraft, freezing fog and FZDZ are both reported as FZDZ.

## 6.2 CANADIAN AIRPORT NOWCASTING FORECAST SYSTEM

The Canadian Airport Nowcasting Forecast System (CAN-Now) is a nowcasting system designed for improved short-term forecasting of all-season weather hazards affecting the terminal area [56]. Weather phenomena include snow and rain; freezing precipitation and ice pellets; frost; blowing snow; icing aloft; high winds and gusts; wind shifts; wind shear; turbulence; lightning; low ceilings and visibility; and fog and convection.

The prototype system has run for several years in a nowcasting mode, detecting weather hazards and providing forecasts to 3–6 hours for most phenomena, and to 36 hours for a subset. Prototype nowcasts rely on existing, routinely-available weather information, including NWP model output; site climatologies; radar and lightning network observations; and measurements from on-site sensors (e.g., wind, precipitation, visibility, ceiling, and temperature), augmented by other specialized information from high-resolution local area models and from high time-resolution instrumentation, such as microwave radiometers, vertically pointing radars, and particle-type sensors. CAN-Now ingests and integrates data from these sources and applies scientifically based algorithms to produce aviation-related parameters (see figure 26). A radar extrapolation scheme moves radar echoes forward based on the history of their past motions to provide a ~2-hour nowcast of precipitation at the airport. The system predicts the most likely precipitation rate and a possible maximum amount (see figure 27). Time bars are drawn at 10-minute intervals for the first 2 hours and then hourly to 6 hours. Parameters include crosswinds for three runway directions; visibility; ceiling; shear/turbulence; precipitation; thunderstorms and lightning; and icing. An Airport Arrival Rate, CAT, and runway condition (dependent on expected weather, referred to as “weather-only”) are also calculated [56]. Several weighting, bias-correction, and adaptive blending schemes are incorporated into CAN-Now to achieve higher accuracy with short-term forecasts.

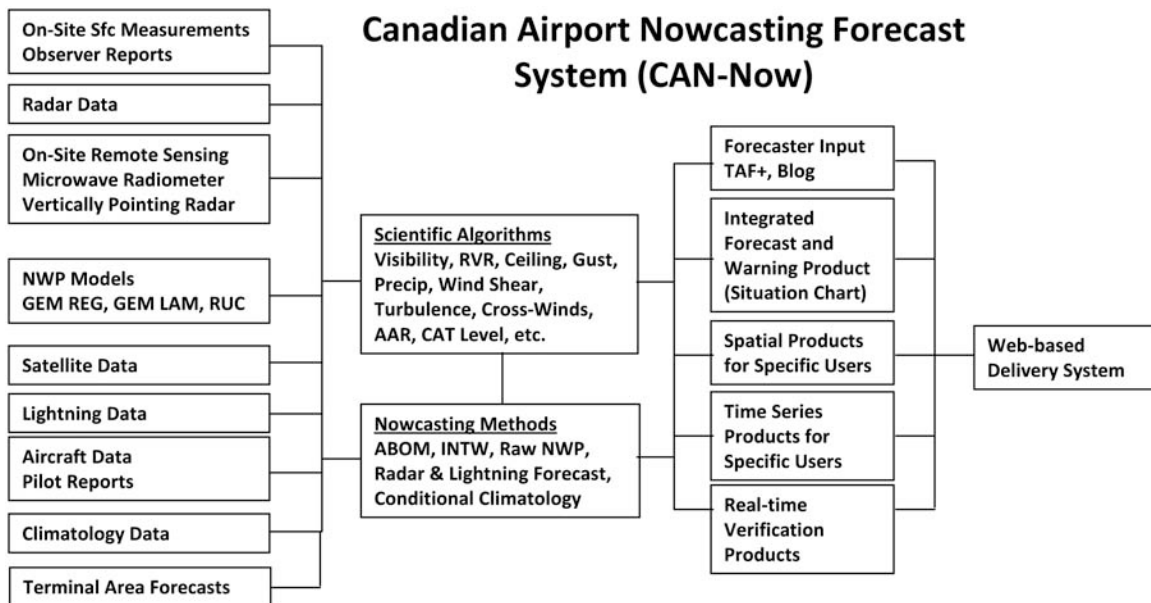
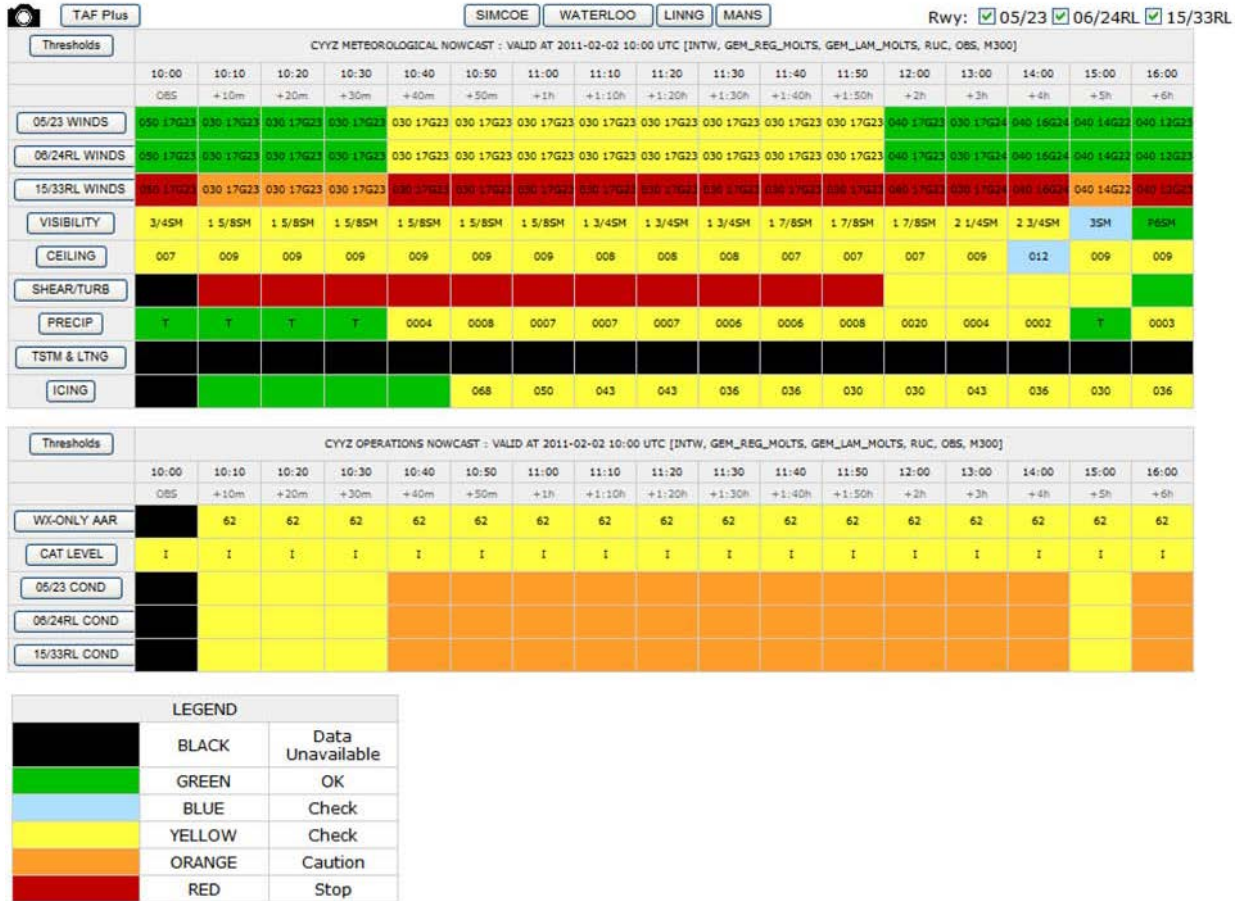


**Figure 26. Schematic of CAN-Now [56]**



Situation Chart for CYYZ



The evaluation of CAN-Now concluded that there is a great deal of future work necessary to more accurately measure precipitation amounts and determine precipitation type [56]. Improvements in the ability to forecast these parameters are also needed. In addition, the current icing aloft forecasts in CAN-Now could be improved through better use of the existing instrumentation (microwave radiometer and vertically pointing radar), newer versions of NWP models that predict liquid water content directly, and incorporation of satellite-based techniques.

7. SUMMARY

Many sensors, both in situ and remote, and forecast and nowcast NWP models and algorithms are currently available for diagnosing icing conditions in the terminal area. Surface-based sensors, such as those found on ASOS, AWOS and AWSS, have the capability to detect icing, either through the use of optical sensors or through direct detection of ice accretion

on vibrating rod instrumentation. Airborne sensors, such as those included with TAMDAR, also detect icing (and no-icing) conditions. Though these systems have proven useful in the detection of icing conditions on the ground and aloft, their measurements are valid only at a single-point. In many cases, particularly at larger airports, icing conditions (e.g., FZDZ) may only affect a portion of the airport or terminal area.

Remote sensors (such as satellite and radar) have the ability to obtain measurements encompassing a much larger area. Significant research has gone into the development of radar- and satellite-based algorithms for detecting icing conditions. Scientists at NASA LaRC have developed algorithms specifically for use with the current weather satellites to determine icing conditions in clouds. Other investigators have been working to develop algorithms for detection of icing and surface-freezing precipitation measurements using radar data, both in their current form and with the NEXRAD dual-polarization upgrades. None of these methods are currently producing NWS or FAA operationally approved products. Though the remote-sensor measurements can provide valuable information for determining icing conditions in the terminal area, they also have their limitations. Satellite products focus on conditions at or near cloud top, whereas radar products are restricted to detecting conditions along the length of the radar beam, which gets higher and broader with distance from the radar.

NWP models can provide information on the ground and aloft, and their resolution can be increased to give better representations of potentially varying icing conditions within the terminal area. As with any other system, though, NWP models have their drawbacks. The higher the resolution of the model, the longer it takes to run the model, often requiring expensive computing resources to provide the forecasts in a timely manner. Models are also highly dependent on their initialization data. If bad data are fed into the model, a bad forecast is likely to be produced. Higher resolution does not necessarily result in better forecasts—the model physics must also be changed to appropriately simulate the weather at those scales. Finally, NWP models are not perfect in their ability to forecast the weather, even with good data being used, and can miss or incorrectly classify the weather in a given area because of the limitations of the model physics. Numerous NWP model forecasts are available. Not all of them provide sufficient resolution in space and time for, nor precipitation types pertinent to, TAIWIN; however, there may be some utility in incorporating their output in an ensemble mode to provide some information on forecast probability or confidence.

Nowcasts, though highly valuable in the short term ( $\leq 1-2$  hours depending on the weather phenomenon), tend to decrease in accuracy in the long term ( $> 2$  hours) because they rely solely on extrapolation and tracking of the current weather and do not account for changing conditions, speed, and weather type.

Various algorithms have been developed to combine relevant information and display it in formats pertinent to their users. These have been adapted to both ground de-icing and inflight icing applications and may provide a good basis for a future TAIWIN.

In summary, all of the capabilities described in this report can help provide information on icing conditions within the terminal area, but none offer a full solution to accurately determine the

location and characteristics of icing conditions at every point within the terminal area. It therefore becomes important to assess the ability of each product to determine the presence, absence, and characteristics of icing conditions and determine how to integrate the products into a single best estimate of icing conditions in the terminal area.

## 8. REFERENCES

1. Krozel, J. and Krishna, S., "Evaluating the Impacts of In-Flight Icing Hazards." *Air Traffic Control Quarterly*, Vol. 19, 2011, pp. 41–61.
2. Ryerson, C.C. and Ramsay, A.C., "Quantitative Ice Accretion Information From the Automated Surface Observing System," *Journal of Applied Meteorology*, Vol. 46, 2006, pp. 1423–1437.
3. Rappa, G., "Medium Intensity Airport Weather System NEXRAD Selection Recommendation," Project Report ATC-311, Prepared for the Federal Aviation Administration, available from NTIS, 2011.
4. Clark, R.A. and Greene, D.R., "Vertically Integrated Liquid Water—A New Analysis Tool," *Monthly Weather Review*, Vol. 100, No. 7, July 1972, pp. 548–552.
5. Smalley, D.J., "Evaluation of Potential of NEXRAD Dual Polarization Products," Report prepared for the Federal Aviation Administration, available through the National Technical Information Service, Springfield, Virginia, 2007.
6. Elmore, K.L., "The NSSL Hydrometeor Classification Algorithm in Winter Surface Precipitation: Evaluation and Future Development," *Weather and Forecasting*, Vol. 26, No. 5, October 2011, pp. 756–765.
7. Zhang, J., Howard, K., and Gourley, J.J., "Constructing Three-Dimensional Multiple Radar Reflectivity Mosaics: Examples of Convective Storms and Stratiform Rain Echoes," *Journal of Atmospheric and Oceanic Technology*, Vol. 22, 2005, pp. 30–42.
8. Zhang, J., Howard, K., and Wang, S., "Single Radar Cartesian Grid and Adaptive Radar Mosaic System. Preprints," *The 12th Conference on Aviation, Range, and Aerospace Meteorology*, Atlanta, Georgia, 2006.
9. Kropfli, R.A., Matrosov, S.Y., Uttal, T., et al., "Cloud Physics Studies With 8 mm Wavelength Radar," *Atmospheric Research*, Vol. 35, 1995, pp. 299–313.
10. Martner, B.E. and Kropfli, R.A., "Observations of Multi-Layered Clouds Using K-Band Radar," Paper AIAA 93-0394, *31st Aerospace Sciences Meeting and Exhibit*, Reno, Nevada, American Institute of Aeronautics and Astronautics., Washington, D.C, January 11–14, 1993.

11. Hogg, D.C., Guiraud, F.O., Snider, J.B., Decker, M.T., and Westwater, E.R., "A Steerable Dual-Channel Microwave Radiometer for Measurements of Water Vapor and Liquid Water in the Troposphere," *Journal of Climate and Applied Meteorology*, Vol. 22, 1983, pp. 789–806.
12. Solheim, F., Godwin, J.R., Westwater, E.R., et al., "Radiometric Profiling of Temperature, Water Vapor and Cloud Liquid Water Using Various Inversion Methods," *Radio Science*, Vol. 33, March-April, 1998, pp. 393–404.
13. Popa Fotino, I.A., Schroeder, J.A., and Decker, M.T., "Ground-Based Detection of Aircraft Icing Conditions Using Microwave Radiometers," *IEEE Transactions on Geoscience and Remote Sensing*, Vol. GE-24, No. 6, 1986, pp. 975–982.
14. Stankov, B.B., Westwater, E.R., Snider, J.B., and Weber, R.L., "Remote Measurements of Supercooled Integrated Liquid Water During WISP/FAA Aircraft Icing Program," *Journal of Aircraft*, Vol. 29, No. 4, July-August, 1992, pp. 604–611.
15. Mecikalski, J.R., Feltz, W.F., Murray, J.J., et al., "Aviation Applications for Satellite-Based Observations of Cloud Properties, Convection Initiation, In-Flight Icing, Turbulence and Volcanic Ash," *Bulletin of the American Meteorological Society*, Vol. 88, 2007, pp. 1589–1607.
16. Minnis, P., Smith, W.L., Jr., Nguyen, L., et al., "Near-Real Time Cloud Properties and Aircraft Icing Indices From Geo and Leo Satellites," *Proceedings of 49th SPIE Annual Meeting, Earth Observing Systems IX Conference*, Denver, Colorado, August 2–6, 2004.
17. Chang, F.-L., Minnis, P., Lin, B., Khaiyer, M., Palikonda, R., and Spangenberg, D., "A Modified Method for Inferring Upper Cloud Top Height Using the GOES-12 Imager 10.7- and 13.3- $\mu\text{m}$  Data," *Journal of Geophysical Research*, Vol. 115, Issue 210, 2010.
18. Smith W.L., Minnis, P., Fleeger, C., et al., "Determining the Flight Icing Threat to Aircraft With Single-Layer Cloud Parameters Derived From Operational Satellite Data," *Journal of Applied Meteorology and Climatology*, Vol. 51, 2012, pp. 1794–1810.
19. Phan, D., Spangenberg, D.A., Palikonda, R., et al., "Web-Based Satellite Products Database for Meteorological and Climate Applications," *Proceedings of 13th AMS Conference on Satellite Oceanography and Meteorology*, Norfolk, Virginia, September 20–24, 2004, CD-ROM, P7.1.
20. Haggerty, J., Vivekanandan, J., and Serke, D., "Evaluation of Satellite and Radar Cloud Retrieval Methods During IMPROVE-2 Icing Events," Paper 8.9, *11th Conference on Aviation Range and Aerospace Meteorology*, Hyannis, Massachusetts, October 4–8, 2004.

21. Black, J., McDonough, F., Haggerty, J., et al., "Comparison of NASA-Langley Satellite-Derived Cloud Top Microphysical Properties With Research Aircraft Data," Paper A5.3, *Proceedings, AMS 23rd International Conference on Interactive Information and Processing Systems for Meteorology, Oceanography, and Hydrology.*, San Antonio, Texas, January 15–18, 2007.
22. Politovich, M., Minnis, K.P., Johnson, D.B., et al., "Benchmarking In-Flight Icing Detection Products for Future Upgrades," Paper 8.10, *Proceedings, AMS 11th Conference on Aviation, Range, and Aerospace Meteorology*, Hyannis, Massachusetts, October 4–8, 2004.
23. Bernstein, B.C., McDonough, F., Wolff, C.A., et al., "The New CIP Icing Severity Product," Poster P9.5, *12th AMS Conference on Aviation, Range and Aerospace Meteorology*, Atlanta, Georgia, January 18–21, 2006.
24. Curry, J.A., Ardeel, C.D., and Tian, L., "Liquid Water Content and Precipitation Characteristics of Stratiform Clouds as Inferred From Satellite Microwave Measurements," *Journal of Geophysical Research*, Vol. 95, No. D10, September 20, 1990, pp. 16,659–16,671.
25. Curry, J.A. and Liu, G., "Assessment of Aircraft Icing Potential Using Satellite Data," *Journal of Applied Meteorology and Climatology*, Vol. 31, No. 6, June 1992, pp. 605–621.
26. Deeter, M.N. and Vivekanandan, J., "Retrievals of Liquid Water Path Based on Amsr-E Observations During AIRS II," Paper 7B.2, *12th AMS Conference on Aviation, Range and Aerospace Meteorology*, Atlanta, Georgia, January 18–21, 2006, available at [http://ams.confex.com/ams/Annual2006/techprogram/paper\\_104647.htm](http://ams.confex.com/ams/Annual2006/techprogram/paper_104647.htm) (last accessed November 2015).
27. Key, J.R. and Intrieri, J.M., "Cloud Particle Phase Determination With the AVHRR," *Journal of Applied Meteorology and Climatology*, Vol. 39, 2000, pp. 1797–1804.
28. Stephens, G.L., Vane, D.G., Boain, R.J., et al., "The CloudSat Mission and the A-Train: A New Dimension of Space-Based Observations of Clouds and Precipitation," *Bulletin of the American Meteorological Society*, Vol. 83, No. 12, December 2002, pp. 1771–1790.
29. Wolff, C.A., Lee, T.F., Mitrescu, C., Landolt, S., and Miller, D.D., "Using CLOUDSAT Data to Validate Icing Products," Paper P4.11, *Proceedings, AMS 13th Conference on Aviation, Range, and Aerospace Meteorology*, New Orleans, Louisiana, January 21–25, 2008.
30. Cornman, L.B., Morse, C.S., and Cuning, G., "Real-Time Estimation of Atmospheric Turbulence Severity From In-Situ Aircraft Measurements," *Journal of Aircraft*, Vol. 32, 1995, pp. 171–177.

31. Daniels, T.S., Tsoucalas, G., Anderson, M., et al., “Tropospheric Airborne Meteorological Data Reporting (TAMDAR) Sensor Development,” Paper 7.6, *11th Conference on Aviation Range and Aerospace Meteorology*, Hyannis, Massachusetts, October 4–8, 2004.
32. Murray, J.J., Schaffner, P.R., Minnis, P., et al. “The 2003 Alliance Icing Research Study (AIRS II) Evaluation of Tropospheric Airborne Meteorological Data Reporting (TAMDAR) Icing Sensor,” Paper 8.5, *11th Conference on Aviation Range and Aerospace Meteorology*, Hyannis, Massachusetts, October 4–8, 2004.
33. Stankov, B.B. and Bedard, A.J., Jr., “Remote Sensing Observations of Winter Aircraft Icing Conditions: A Case Study,” *Journal of Aircraft*, Vol. 31, No. 1, January-February 1994, pp. 79–89.
34. Politovich, M.K., Stankov, B.B., and Martner, B.E., “Determination of Liquid Water Altitudes Using Combined Remote Sensors,” *Journal of Applied Meteorology and Climatology*, Vol. 34, 1995, pp. 2060–2075.
35. Stankov, B.B., Martner, B.E., and Politovich, M.K., “Moisture Profiling of the Cloudy Winter Atmosphere Using Combined Remote Sensors,” *Journal of Atmospheric and Oceanic Technology*, Vol. 12, 1995, pp. 488–510.
36. Reehorst, A.L., Brinker, D.J., and Ratvasky, T.P., “NASA Icing Remote Sensing System: Comparisons From AIRS-II. NASA/TM-2005-213592,” 2005.
37. Johnston, C., Serke, D., Adriaansen, D., et al., “Comparison of In-Situ, Model and Ground Based In-Flight Icing Severity,” AMS Preprint, Seattle, Washington, January 24–27, 2011.
38. Reehorst, A., Politovich, M.K., Zednik, S., Isaac, G.A., and Cober, S., “Progress in the Development of Practical Remote Detection of Icing Conditions (NASA/TM 2006-214242),” NASA, 2006.
39. Serke, D.J., Hubbert, J., Ellis, S., et al. “The Winter 2010 FRONT/NIRSS In-Flight Icing Detection Field Campaign,” *AMS 35th Conference on Radar Meteorology*, Pittsburgh, Pennsylvania, September 26–30, 2011.
40. NOAA, “Earth System Research Laboratory Rapid Refresh (RR),” available at <http://rapidrefresh.noaa.gov> (last accessed August 2015).
41. Zhou, B., Du, J., Manikin, G., and DiMego, G., “Introduction to NCEP’s Time Lagged North American Rapid Refresh Ensemble System (NARRE-TL),” presented at the *15th Conference on Aviation, Range and Aerospace Meteorology*, Los Angeles, California, August 1–4, 2011.
42. Politovich, M.K., “Predicting Inflight Aircraft Icing Intensity,” *Journal of Aircraft*, Vol. 40, No. 4, 2003, pp. 639–644.

43. Bernstein, B.C., McDonough, F., Politovich, M.K., et al., “Current Icing Potential: Algorithm Description and Comparison With Aircraft Observations,” *Journal of Applied Meteorology and Climatology*, Vol. 44, 2005, pp. 969–986.
44. McDonough, F., Bernstein, B.C., Politovich, M.K., and Wolff, C.A., “The Forecast Icing Potential Algorithm,” Paper AIAA 2004-231, *42nd AIAA Aerospace Sciences Meeting and Exhibit*, Reno, Nevada, January 5–8, 2004.
45. Fowler, T.L., Chapman, M., Holmes, A., et al., “Quality Assessment Report Current Icing Potential (CIP): Probability, Severity, and SLD,” report to the FAA AWRP Technical Review Panel, 2006.
46. Bernstein, B.C., Wittmeyer, I., and Hirvonen J., “LOWICE: An Example of the Adaption of In-Flight Icing Diagnosis Concepts to the Structural Icing Environment,” Paper 2011-38-0070, *SAE 2011 International Conference on Aircraft and Engine Icing and Ground Deicing*, Chicago, Illinois, June 13–17, 2011.
47. Albers, S., McGinley, J., Birkenheuer, D., and Smart, J., “The Local Analysis and Prediction System (LAPS): Analyses of Clouds Precipitation, and Temperature,” *Weather and Forecasting*, Vol. 11, 1996, pp. 273–287.
48. Le Bot, C., “SIGMA: System of Icing Geographic Identification in Meteorology for Aviation,” Paper 6.5, *AMS 11th Conference on Aviation Range, and Aerospace Meteorology*, Hyannis, Massachusetts, October 4–8, 2004.
49. LeBot, C., Page, C., and Drouin, A., “SIGMA: Diagnosis and Nowcasting of In-Flight Icing—Improving Aircrew Awareness Through FLYSAFE,” Paper 13.2, *Proceedings of AMS 13th Conference on Aviation, Range, and Aerospace Meteorology*, New Orleans, Louisiana, January 21–25, 2008.
50. Chapman, M., Pocerlich, M., Holmes, A. et al., “Quality Assessment Report: Forecast Icing Product (FIP)—Severity,” report to the FAA AWRP Technical Review Panel, 2006.
51. Chapman, M., Holmes, A., and Wolff, C. “Verification of Aviation Icing Algorithms From the Second Alliance Icing Research Study,” Paper 7.B3, *AMS 12th Conference on Aviation Range, and Aerospace Meteorology*, Atlanta, Georgia, January 30–February 2, 2006.
52. Tafferner, A., Hauf, T., Liefeld, C., et al., “ADWICE: Advanced Diagnosis and Warning System for Aircraft Icing Environments,” *Weather and Forecasting*, Vol.18, 2003, pp. 184–203.
53. Forbes, G.S., Hu, Y., Brown, B.G., Bernstein, B.C., and Politovich, M.K., “Examination of Conditions in the Proximity of Pilot Reports of Aircraft Icing During STORM-FEST,” Preprints, *AMS 5th International Conference on Aviation Weather Systems*, Vienna, Virginia., August 2–6, 1993, pp. 282–286.

54. Tendel, J. and Wolff, C., “Verification of ADWICE In-Flight Icing Forecasts: Performance vs. PIREPS Compared to FIP,” Paper 2011-38-0068, *SAE 2011 International Conference on Aircraft and Engine Icing and Ground Deicing*, Chicago, Illinois, June 13–17, 2011.
55. Rasmussen, R., Dixon, M., Hage, F., et al., “Weather Support to Deicing Decision Making (WSDDM): A Winter Weather Nowcasting System,” *Bulletin of the American Meteorological Society*, Vol. 82, 2011, pp. 579–595.
56. Isaac, G., Bailey, M., and Boudala, F., “Decision Making Regarding Aircraft De-Icing and Inflight Icing Using the Canadian Airport Nowcasting System (CAN-Now),” Paper 2011-38-0029, *SAE 2011 International Conference on Aircraft and Engine Icing and Ground Deicing*, Chicago, Illinois, June 13–17, 2011.